DUACS DT2014 : the new multi-mission altimeter dataset reprocessed over 20 years

M.-I. Pujol[1*], Y. Faugère[1*], G. Taburet[1], S. Dupuy[1], C Pelloquin[1], M. Ablain[1], N. Picot[2]

[1]{Collecte Localisation Satellites, Toulouse, France}

[2]{Centre National Etudes Spatiales, Toulouse, France}

[*]{M.-I. Pujol and Y. Faugere contributed equally to this paper}

Correspondence to: M.-I. Pujol (mpujol@cls.fr)

Abstract

The new DUACS DT2014 reprocessed products have been~~are~~ available since April 2014. Numerous innovative changes~~and impacting evolutions~~ have been introduced~~implemented~~ at each step of an extensively~~this~~ revised~~new~~ data processing protocol. ~~The main one~~An ~~impacting change for users is t~~The use of a new 20-year altimeter reference period in place ~~,~~ ~~instead~~of the previous 7-year ~~-~~reference~~,~~ ~~that~~ significant~~strong~~ly ~~changes~~ changes~~d~~ the SLA ~~and SLA gradient signature~~patterns and thus will have a strong user ~~ly~~ impact~~ed the users~~. ~~Other changes implemented directly contributed to improve the DT2014 SLA quality. They consist in using~~ The use of up to date altimeter standards and geophysical corrections, reduced smoothing of the along-track data, and refined mapping parameters, including spatial and temporal correlation scale~~s~~ refinement~~definition~~ and measurement errors all contribute to an improved high quality ~~the~~ DT2014 SLA dataset~~quality~~. Although all of the DUACS products have been upgraded~~improved~~, this paper focuses on the enhancements to the gridded SLA products ~~quality description~~ over the global ocean. As part of~~as~~ this exercise, 21 years of data have been homogenized allowing us to retrieve accurate large scale climate signals such

as global and regional MSL trends, ~~as well as~~ interannual signals, and better ~~but also~~ refined mesoscale features.

An e~~E~~xtensive assessment exercise has been carried out~~performed~~ on this dataset, which allows~~ed~~ us to establish a consolidated error budget. The errors at mesoscale are about 1.~~5cm~~4cm² in low variability areas, ~~and~~ increase to an average of 8.9~~9~~cm² ~~in average~~ in coastal regions, and~~to~~ reach ~~more than~~nearly 32.5~~0~~cm² in high mesoscale activity areas. The DT2014 products, compared to the previous DT2010 version ~~DT2010~~, present~~s~~ additional signals for wavelengths lower than ~250 km, inducing SLA variance and mean EKE increases of respectively +5.1% and +15%. Comparisons with independent measurements ~~underlined~~ highlight~~ed~~ the improved mesoscale~~s~~ ~~restitution~~ representation within this new dataset. The error~~s~~ reduction at the mesoscale reaches nearly 10% of the error observed with DT2010. ~~The~~ DT2014 also presents an improved coastal signal with a nearly 2 to 4% mean error reduction. High latitude~~s~~ areas are also ~~better~~ more accurately represented in DT2014, with an ~~better~~ improved consistency between ~~map~~ spatial coverage and sea ice edge position. An error~~The~~ budget ~~error~~ is used to~~finally discussed, in order to~~ highlight the limitations of the new gridded products, with notable errors~~notably~~ in areas with strong internal tides~~ area~~.

1 Introduction

Since its inception~~beginning~~ in late 1997, the DUACS (Data Unification and Altimeter Combination System) system has ~~aims at~~ produced~~ing~~ and delivered~~ing~~ high quality along track (L3 products) and multi-mission gridded (L4 products) altimeter products that are used~~directly usable~~ by a large variety of users ~~and~~ for different applications. The~~y~~ data are available~~delivered~~ both in Near Real Time (NRT), with a delay of a ~~comprised betwee~~few hours to one day, and in a Delayed Time (DT) mode where there is a complete~~ly~~ reprocessing~~ed~~ ~~about~~ every ~~three~~ four years~~ thanks to a Delayed Time (DT) mode~~. Over~~During~~ the last two decades, successive papers have described the evolution of the DUACS system and its associated products (Le Traon et al, 1992; 1995; 1998; 1999; 2003; Ducet et al, 2000; Pujol et al, 2005; Dibarboure et al., 2011). T~~In overall, t~~he quality of DUACS products ~~quality~~ is affected~~impacted~~ by several factors, such as the altimeter~~ry~~

constellation used for~~in~~ input (Pascual et al, 2006; Dibarboure et al, 2011), the choices of ~~the~~ altimeter~~s~~ standards (Dibarboure et al, 2011; Ablain et al, 2015), and ~~the~~ improvements in ~~of the~~ data processing algorithms (Ducet et al, 2000; Dussurget et al, 2011; Griffin et al, 2012; Escudier et al, 2013).

This paper addresses~~is dedicated to~~ a~~the~~ new global reprocessing that covers the entire altimeter period and allows us, for the first time, to generate a gridded ~~product~~ time series of more than 20 years, identified here as DT2014. The period starts at the beginning of the altimeter era and ranges from 1993 to 2013. Measurements from 10 altimeter~~s~~ missions (~~repetitive~~ repeat track and geodetic orbits) have been used : the TOPEX/Poseidon (TP) and Jason series (Ja~~n~~son-1 (J1) & Jason-2 (J2)), ERS-1/2 and ENVISAT (EN), Geosat Follow On (GFO), Cryosat-2 (C2), AltiKa (AL) and Haiyang-2A (HY-2A). DT2014 represents a major~~It~~ upgrade of~~s~~ the previous version, ~~(called~~ DT2010 (~~;~~ Dibarboure et al., 2011), but ~~and still~~ pursues the same objectives that comprise the~~first consist in~~ generation of~~ng~~ time series that are~~as~~ homogeneous in terms of altimeter standards and processing ~~and up to date as possible and in providing in a gridded product containing a large panel of~~~~different~~with an optimal content at both ~~ocean signals from the~~ mesoscales ~~to the~~and ~~ocean climate~~ large scales. To achieve this objective, various algorithms and corrections developed by~~in~~ the research community and through different projects and programs as the French SALP/~~AVISO~~Aviso, the European Myocean2, and the European Space Agency (ESA) Climate Change Initiative projects. The development of regional experimental DUACS products in the framework of scientific oceanographic campaigns such as KEOPS-2 (d'Ovidio et al, 2015) was also valuable for local ~~to~~assessments of ~~locally~~ the improvements, prior to the~~before the~~ implementation and release of ~~in~~the global product. However, one of the main priorities was to improve the monitoring of the mesoscales in the global ocean. Indeed, recent papers (Dussurget et al, 2011, Chelton et al, 2011, Escudier at al. 2013) have shown that despite the accuracy of the DT2010 gridded products, the interpolation of mesoscale signals ~~interpolation is~~are limited by the anisotropy of the altimetry observing system, and finer scale signals contained in the altimeter raw measurements are not really exploited and provided in the higher level DUACS products (L3 and L4). In addition to these mesoscale~~s~~ retrieval improvements and to satisfy the needs of ~~the large panel~~different ~~the~~ ~~AVISO~~Aviso~~'s~~ users, the new DT2014 reprocessing product also benefits~~ciated~~ from climate standards and corrections that do not degrade the mesoscale signals. Thus, the different choices and trade-offs that have been made in the~~ decided to~~ generation of~~e~~ the DT2014 reprocessing are described in detail~~s~~ in this paper.

The DT2014 reprocessing is characterized by important changes in terms of altimeter standards, data processing and formats. The main changes consist of~~in~~ referencing the SLA products to~~on~~ a new altimeter reference period, taking advantage of the 20 years of measurements that are currently available; optimizing ~~the~~ along-track random noise reduction, which affected ~~when~~ ~~in the DT2010 version~~ a large part of the physical signal in the DT2010 version~~was impacted by this processing~~. These changes make~~It results~~ a significant~~important~~ impact on~~in~~ the physical content of the SLA and ~~derivated~~derived products. The gridded SLA products are constructed using more accurate parameters (e.g., correlation scales, error budgets), and computed directly at~~on~~ the 1/4°x1/4° Cartesian grid resolution. Other changes that have been implemented allow~~ed~~ us to correct a number of different anomalies that were detected i~~o~~n the previous DT2010 product suite~~s~~. The resulting quality of the sea surface height estimate ~~and current products~~ is improved. ~~We present i~~In this paper we introduce DT2014, the~~is~~ latest~~st~~ version of the Aviso ~~DT2014~~ SLA product range, ~~s~~ and evaluate its ~~its~~ improvements with respect ~~compared~~ to the previous version.

The paper is organized as follows: ~~the~~ details of the ~~altimeter~~ L3/L4 -altimeter data processing used for the generation of the DT2014 products ~~generation~~, ~~with changes implemented in the DT2014 products,~~ is presented in section 2. In section 3~~3~~, results obtained from the DT2014 SLA reprocessed products are compared with equivalent DT2010 results, focusing on the mesoscales and coastal areas. In the same section, ~~we give~~ for the first time, we make an estimate~~ion~~ of the L4 SLA product errors. Finally, a summary of the key results obtained are given in section 4~~4~~.

2 Data Processing

2.1 Altimeter standards

The altimeter standards used for~~in~~ DT2014 were selected taking advantage of the work performed during~~in~~ the first phase of the Sea Level Climate Change Initiative (SL_cci) led by the Eu~~t~~rop~~o~~ean Space Agency in 2011-2013. The objective of this~~is~~ project was~~aimed~~ to generate ~~the~~ optimal reprocessed products for climate applications, notably global and regional mean sea level trends. As part of this exercise, a rigorous selection process was put~~set~~ in place. This process, as well as all the selected standards~~ selected~~, is described by~~in~~ Ablain et al. (~~,~~2015). As recommended by the SL_cci project, ~~two~~ several major standards were implemented~~changed~~ in the DT2014 products, compared to ~~the~~ DT2010.~~ First, new orbit solutions were used: GDR-D (or equivalent) standards for Envisat, Jason-1, Jason-2 and Cryosat, and REAPER solution (Rudenko et al, 2012) for ERS-1 and ERS-2. Then, the ERA Interim reanalyzed atmospheric fields were used in the Dynamic Atmospheric Correction and dry troposphere corrections.~~

One of the most dramatic improvements comes from the use of ERA-interim reanalys~~i~~es (from the European Centre for Medium-Range Weather Forecasts -ECMWF-; Dee et al., 2011) instead of operational ECMWF fields for the~~to~~ calculation of~~e~~ the dry tropospheric and other dynamical atmospheric corrections. Important~~A strong~~ improvements have been observed over the first altimetry decade (1993-2003) -at the mesoscale and, especially, at high latitudes, allowing a better estimation of ~~the~~ long-term regional mean sea level trends (Carrere et al., 2016) with for instance, ~~an~~ impacts higher than 1 mm/yr in the South Pacific Ocean below 50°S latitude. However, t~~T~~he evaluations also showed that the use of this correction slightly degraded the mesoscale signals for~~on~~ the second altimetry decade. To e~~i~~nsure an optimal description of these signals for~~to~~ Aviso/Myocean-2 users, the Operatio~~n~~nal ECMWF fields were used from 2001 onwards.

Another major~~strong~~ improvement has been achieved by~~carried out~~ using new orbit solutions for all of the altimeter missions: REAPER combined orbit solutions (Rudenko et al., 2012) for ERS-1 and ERS-2, CNES GDR-D orbit solutions (Couhert et al., 20145) for the Jason-1, Jason-2 and Envisat missions. Significant~~Strong~~ effects were observed on ~~the~~ regional sea level trends, in the range ~~of~~ 1-2 mm/yr, with large patterns at hemispheric scale when using static and time variable Earth gravity field models for orbit computation. Thanks to cross-comparisons between altimetry missions (Ollivier et al., 2012) and with in-situ measurements (Valladeau et al., 2012), ~~it has been demonstrated that~~ these new orbit solutions have been demonstrated to dramatically improve~~d~~ the regional sea level trends.

In addition to these major improvements, other new altimeter standards were also selected, although their impacts on ~~the~~ sea level estimates was lower. These mainly concern the radiometer-based corrections that use~~using~~ combined estimates from valid on-board MWR values and Global Navigation Satellite System~~s~~ (GNSS) measurements (Fernandes et al., 2015) and the ~~the~~ ionospheric correction with the use of the NIC09 (New Ionosphere Climatology) model for ERS-1 (Scharroo et al., 2010).

~~In the Aviso/Myocean-2 context, we also needs to insure an optimal restitution retrieval of the mesoscale signal, some adjustments in the standards selection were done. Notably, whereas the ERA Interim reanalysis based corrections are considered over the whole altimeter period in the SL_cci project, we used it only during the first decade (i.e. for TP, ERS-1/2) in the DUACS products. Indeed, evaluations done within SL_cci project (Carrere et al. (2015); Ablain et al, 2015) clearly underlined showed that the use of ERA-Interim reanalysis based correction (instead of ECMWF operational fields) strongly improves mesoscales and regional spatial scales observation for the first altimetry decade, while not significant improvement is observed from 2004.~~

The details of the altimeter standards used in the DT2014 products are given in ~~AVISO~~Aviso (2014b).

2.2 DUACS DT2014 processing

2.2.1 Overview of the DUACS DT processing

The DUACS DT processing includes different steps as described by Dibarboure et al (2011). The steps ~~y~~ consist of~~in~~ acquisition, homogenization, input data quality control, multi-mission~~s~~ cross-calibration, along-track SLA generation, multi-mission~~s~~ mapping, final quality control and, finally, dissemination of the products. ~~From the along-track and gridded SLA products thus obtained, different derivated products as geostrosphic velocities are also computed.~~ Here ~~W~~we ~~summarizes~~ present ~~here~~ ~~the changes in the different processing steps of the DUACS DT system that have direct impacts on the products accuracy and for the users~~details of the DT2014 processing system and evolution~~s~~ compared to the DT2010 version.~~.~~

Acquisition~~/homogenization~~:

60+ cumulative years of different datasets were acquired over the 21-year period [1993, 2013]. They include measurements from ~~the~~ 10 different altimeters: ERS-1/2, EN (~~repetitive~~ repeat track and geodetic orbits), TP, J1 (~~repetitive~~repeat track orbit, tandem and geodetic end of life orbit), J2, GFO, C2, AL and HY-2A. The different periods covered by the different altimeters is summarized in Fig. 1. The main differences from~~with~~ DT2010 is the introduction of the year 2011 for C2 and the first cycles of the J1 geodetic orbit (cycle 500 to 505, May to mid June 2012).

Input data quality control:

The detection of invalid measurements was based on the traditional approach developed~~set up~~ for DT2010. D~~The d~~etails of this editing exercise are given in Aviso/SALP (2015). It involves~~implies~~ various algorithms, from the simplest, such as ~~like~~ threshold selection for~~on~~ the different parameters, to more complex (e.g., SLA selection with splines). For the DT2014 processing, a more restrictive data selection was applied ~~and was improved~~, ~~on one hand,~~ for ~~non~~ non-~~repetitive~~ repeat track and the new repeat track orbit missions ~~(J1 geodetic, C2)~~that are becoming more~~more and mor~~ prevalent~~present~~ in the reprocessing. ~~, and in the other hand, in new areas as the coastal zone (all the missions) and high latitudes (C2, AL).~~ As these new missions are able to sample the ocean surface in areas never reached before by older~~other~~ altimeters, their data~~y~~ are usually contaminated by the reduced quality of geophysical corrections and Mean Sea Surface (MSS) in these specific areas. Such anomalies were observed in the DT2010 along-track SLA ~~products~~ fields, and were responsible for the introduction of~~introduced~~ anomalies to the~~on~~ gridded ~~products~~fields, especially in coastal and high latitude areas. In order to avoid this problem in the DT2014 products, the criteria used for the detection of erroneous measurements along non-repeat tracks and the new repeat tracks was strongly restricted in coastal areas. Indeed, ~~T~~the measurements along the ~~non repetitive~~ERS-1 (during geodetic phase), EN geodetic, J1 geodetic, C2, and HY-2A orbits are systematically rejected when closer ~~to the coast~~ than 20 km to the coast. In the same way, the poor~~bad~~ quality of the ~~Mean Sea Surface (~~MSS~~)~~ in the Laptev Sea ~~conduces~~ leads to ~~the~~ systematic ~~detection~~ rejection of the measurements along non ~~repetitive~~ repeat track orbits in this area. The use of a MSS to generate SLA along non ~~repetitive~~ repeat track orbits is discussed in the "Along-track SLA generation" paragraph.

Multi-mission homogenization and cross-calibration:

The first homogenization step~~,~~ consists of~~in~~ acquiring ~~the~~ altimeter and ancillary data from the different altimeters that are a priori as homogeneous as possible~~ for the different altimeters~~. The data should~~y~~ include the most recent standards recommended for altimeter products by the different agencies and expert groups such as OSTST, ESA Quality Working groups or ESA SL_cci project. The up to date standards used for DT2014 are described and discussed in ~~the~~ Sect. 2.1.

Although the raw input L2 GDR datasets are properly homogenized and edited (see "*Input data quality control")*, they are not always coherent due to various sources of geographically correlated errors (instrumental, processing, orbit~~s~~ residuals errors). Consequently, the multi-mission cross-calibration algorithm aims to~~at~~ reduce~~ing~~ these errors in order to generate a global, consistent and accurate data~~-~~set for all altimeter~~s~~ constellations.

The second homogenization step, crucial for climate signals, consists of~~in~~ ensuring ~~the~~ mean sea level continuity between the three altimeter reference missions. The DUACS DT system uses, first, TP from 1993 to April 2002, then J1 until October 2008 and, finally, J2 that covers the end of the period. This processing step consists of~~in~~ reducing the global and regional biases for each transition (T/P-J1 and J1-J2), using the calibration phase of the J1 and J2 altimeters where the altimeters follow~~are on~~ the same orbit~~,~~ with a few hours ~~of~~ phase offset. Thus, a first polynomial adjustment allows ~~to~~ reduction of~~e~~ the latitude depende~~a~~nt biases between the two successive reference missions, as well as the global mean bias observed between the two successive missions. A second adjustment consists of~~in~~ reducing ~~the~~ regional long wavelength residual biases. As illustrated i~~o~~n Fig. 2, this adjustment ~~it~~ permits ~~to~~ removal of~~e~~ large spatial pattern (basin scale) errors of the order of 1-2 cm.

Next~~Then~~, a cross-calibration process consists of~~in~~ reducing ~~the~~ orbit errors through~~by~~ a global minimization of the crossover differences observed for the reference mission, and between the reference and ~~secondary~~ ~~the~~ other missions also identified as complementary and opportunity missions (i.e. TP after April 2002, J1 after Oct. 2008, ERS-1, ERS-2, EN, GFO, AL, C2 and HY-2A). ~~No specific change was implemented for this step of the processing in the reprocessed version.~~The methodology, used ~~is the same as~~ also for DT1010 dataset~~. It~~ is described ~~by~~by~~in~~ Le Traon and Ogor (1998).

The last step consists of~~to~~ applying the long wavelength error~~s~~ ~~(LWE)~~ reduction algorithm. This process reduces ~~the~~ geographically-correlated errors between neighboring tracks from different sensors. This optimal-interpolation based empirical correction ~~based on optimal interpolation~~ (~~Le Traon et al. 1998, Ducet et al., 2000~~Appendix B) also contributes to reduction of~~e~~ the residual high frequency signal that is not fully corrected by~~with~~ the different corrections that are applied (mainly the Dynamic Atmospheric Correction and Ocean tides). This empirical processing requires~~need~~ an accurate description of the variability of the error signal associated with~~to~~ the different altimeter missions. The variance of the correlated long-wavelength errors used in the DT2014 processing is described in the "*Multi-mission mapping*" paragraph. ~~In the DT2014 products, the long-wavelength residual ionosphere signal, that can be observed when this correction is deduced from a model (typically for mission with mono-frequency measurement), is taken into account for ERS-2, C2 and HY-2A. In the same way, geodetic missions, for which no precise mean profile is available (see hereafter), present additional long-wavelength errors induced by the use of a global gridded Mean Sea Surface for SLA computation. These MSS additional errors were taken into account in the reprocessed products for C2, J1 geodetic phase, EN on it geodetic orbit and HY-2A.~~

Along-track SLA generation:

In order to take advantage of the repeat~~titive~~ characteristics of some altimeter missions, and to facilitate~~ease the~~ use of altimeter products by the users, the measurements are co-located onto theoretical positions, allowing us to estimate a precise Mean Sea Surface (MSS) along these~~es~~ tracks; The MSS is~~,~~ also referred to as the~~named~~ Mean Profile (MP). The MPs are time averages of the co-located Sea Surface Height (SSH) measured by the altimeters with repeating~~titive~~ orbits. The DT2014 reprocessing includes the reprocessing of these MPs along the TP/J1/J2, TP-tandem/J1-tandem, ERS-1/ERS-2/EN and GFO tracks. The MPs ~~Indeed, they~~ need to be consistent with the altimeter standards ~~used~~ (see Sect. 2.1), and the MSS that is~~also~~ used for the non ~~repetitive~~ repeat track orbit missions. ~~The~~ MP reprocessing includes~~d~~ specific attempts~~efforts~~ to improve ~~the~~ accuracy and extend the~~ir~~ estimates~~ion~~ into the high latitudes areas. One of the main changes included in the new~~is~~ MPs~~s~~ reprocessing is the use of a new 20-year [1993, 2012] altimeter reference period, as more fully~~better~~ explained in Sect. 2.2.2. Additionally, the precision of the different MPs was improved by combining ~~the~~ altimeter data that are on the same orbit. In this way, TP, J1 and J2 measurements are all used to define the corresponding MP; TP tandem and J1 tandem or ERS-2 and EN are also merged. This processing leads to an improved definition of the MPs~~ near the coast,~~ with, in particular, a gain of defined positions near ~~from~~ the coast. The number of points defined within 0-15 km ~~far~~ from the coast in the new~~est~~ MPs is ~~indeed~~ twice (three times) the number observed in the previous MP version~~ of the MPs~~, ~~respectively~~ along respective TP and TPN theoretical tracks. In the same way, an additional 15 to 20% more points are defined near the coasts~~,~~ along the GFO and EN theoretical tracks in the new~~est~~ MPs. The MP along EN theoretical tracks is also ~~better~~ more accurately defined in the high latitude~~s~~ areas, taking advantage of increased~~the more important~~ ice melt since~~occurring after year~~ 2007 (Fig. 3).

In the case of the non repeating~~tive~~ missions (i.e., ERS-1 during the geodetic phase; EN after the orbit change; J1 on the geodetic phase; C2), or recent missions following the~~a~~ newest theoretical track (i.e., HY-2A), the estimation of a precise MP is not possible. In this~~at~~ case, the SLA is estimated along the real altimeter tracks, using a gridded MSS as a reference. The latter is the MSS_CNES_CLS_11 described by Schaeffer et al (2012), and corrected in order to be representative of the 20-year [1993, 2012] period (see also Sect. 2.2.2).

The SLA, obtained by subtracting the MP or MSS from~~on~~ the SSH measured by the altimeter, is affected by measurement noise~~s~~. A Lanczos low pass along-track filtering allows us to reduce this noise. Two different filtering parameterizations are used, according to the application. For the generation of the L3 along-track ~~products~~SLA, the cut-off wavelength was revisited in the DT2014 in order to reduce ~~as much as possible the~~ random measurement noise as much as possible whilst~~,~~ retain~~keep~~ing ~~safe~~ the dynamic signal. More details are given in ~~Sect. 2.2.3.in order to keep one point over two, leading to a nearly 14km distance between two successive points. Because some applications need the full resolution data, the non-filtered and non-sub-sampled products are also distributed in DT mode.~~ ~~in~~ the following section. ~~.~~For the generation of the L4 gridded SLA, the filtering is also intended~~aims~~ to reduce small~~short~~ scale dynamical signals that cannot be accurately retrieved. Details are given in~~s~~ Sect. *Multi-mission mapping.*

Along track noise filtering

The gridded product~~s~~ processing parameters are~~is~~ a trade-off between the altimeter constellation sampling capability and the signal to be retrieved. For DT2010~~,~~ the processing~~,~~ and, in particular, the along track noise filtering were~~was~~ set up in accordance with~~to~~ this objective. Consequently, the global DT2010 along-track SLA products were low-pass filtered with a Lanczos cut-off filter with wavelengths depending on latitude (250 km near the e~~E~~quator, down to~~until~~ 60 km at high latitudes). This technical choice was mostly linked to the ability of the TP altimeter mission to capture ocean dynamic~~s~~ mesoscale structures (Le Traon and Dibarboure 1999). However it ~~reduced~~ strongly reduced the along-track resolution, that can~~might~~ be useful and beneficial for~~to~~ modeling and forecasting systems. For this reason~~That is why~~ a dedicated along track product that~~,~~ preserves the along track 1 Hz high resolution signals has been developed in the frame of the DT2014 reprocessing. The main inputs come from the study by Dufau et al. (2016).

An SLA power spectrum density analysis was used in order to determine the wavelength where signal and error are of the same order of magnitude. It represents the minimum wavelength associated with the dynamical structures that altimetry would statistically be able to observe with a signal-to noise ratio greater than 1. This wavelength has been~~was~~ found to be variable in space and time (Dufau et al., 2016). The mean value was found to be nearly 65 km. It was defined with a single year of Jason-2 measurements, over the global ocean, excluding latitudes between -20°S and 20°N (due, in part, to the limit of the underlying Surface Quasi-Geostrophic turbulence in these areas).~~a singles, for, in part,ie~~ In~~At~~ the end ~~it was retained to use this~~ the cut-off length of 65 km in the DT2014 along-track low-pass filtering processing was retained. It is considered as the minimal low-pass cut-off length that can be applied to~~on~~ along-track SLA in order to reduce noise effects and~~,~~ preserve~~ing~~ as much as possible the physical signal. This~~It~~ however cannot be defined as a perfect noise removal operation since, in practice, a signal-to-noise ratio of 2 to 10 (cut-off with wavelength of 100-150 km or more) would be required to obtain~~get~~ a noise-free topography.

The filtered along-track products are subsampled before~~for~~ delivery in order to retain~~keep~~ every second point along the tracks, leading to a nearly 14 km distance between ~~two~~ successive points. Because some applications need the full resolution data, the non-filtered and non-sub-sampled products are also distributed in DT mode.

Multi-mission mapping:

Before the multi-mission merging into a gridded product, t~~T~~he along-track measurements are also low-pass filtered in view of the mapping process. In this case, the aim of the filtering is also ~~aims~~ to reduce the signature of the short scale~~s~~ signals that cannot be properly ~~mapped~~ retrieved ~~(~~mainly due to limitations of the altimetry spatial and temporal sampling~~)~~. Indeed, the altimeter~~s~~ inter-track~~s~~ diamond~~s~~ distances and the revisit time period limit the observation of mesoscale structures. Previous studies (Le Traon and Dibarboure, 1999; Pascual et al, 2006) underscore~~d~~ the necessity for~~of~~ a minimum of a~~al~~ 2-satellite~~s~~ constellation for the retrieval of~~ing~~ mesoscale signals. Thus, in view of the mapping process, the along-track SLA are low-pass filtered by applying a cut-off wavelength that varies with latitude in order to attenuate SLA variability with wavelengths shorter than nearly 200 km near the equator, and~~to~~ nearly 65 km for latitudes higher than 40°. ~~The wavelengths ranging nearly 200 to 65 km are filtered (latitude dependant).~~ Finally, a~~A~~ latitude dependent sub-sampling~~, is also applied. The sub-sampling rate is latitude dependant,~~ is applied in order to be commensurate with the filtering~~ applied, is finally applied~~. ~~*Finally, the along-track measurements are sub-*~~

~~*sampled in order to keep one point over two, leading to a nearly 14km distance between two successive points. Because some applications need the full resolution data, the non-filtered and non-sub-sampled products are also distributed in DT mode.*~~

~~*Multi-mission mapping:*~~

The objective of the mapping procedure is~~aims~~ to construct a ~~a regularly gridded~~ SLA field on a regular grid by combining measurements from different altimeters. The DUACS mapping processing mainly focuses on mesoscale signal reconstruction. It uses an Optimal Interpolation (OI) processing as described in ~~Ducet et al (2000) and Le Traon et al (2003)~~Appendix B. This methodology requires~~needs~~ a description of the observation errors and of the characteristics of the physical signal that we want to map. The parameters used for the mapping procedure are a compromise between the characteristics of the physical field we focus on, and the sampling capabilities associated with the altimeter constellation~~ sampling capabilities~~. The parameters used in the DT2014 OI processing were optimised~~refined~~.

The main improvements consist of~~in~~ computing the maps with a daily sampling (i.e., a map is computed for each day~~s~~ of the week, while only maps centered on Wednesdays we~~a~~re~~s~~ computed for~~in~~ DT2010). The reader should, however, note that the time scales of the variability that is~~are~~ resolved in the DT2014 dataset are not substantially different from DT2010; these time scales are imposed by the temporal correlation function used in the OI mapping procedure. The temporal correlation scales are discussed later~~after~~ in this section~~chapter.~~. A second important change is the definition of the grid points with a global Cartesian 1/4°x1/4° resolution. This choice was mainly driven by user requests since Cartesian grid~~s~~ manipulation is simpler than~~st~~ working on~~compared to~~ a Mercator projection~~. Compared to the historical 1/3°x1/3° Mercator resolution, the Cartesian projection leads to an improved resolution between latitude of nearly ±41.5°N, as illustrated in (Fig. 4). These latitudes include the main part of the high variability mesoscales areas, like the Gulf Stream, Kuroshio, Agulhas current and North of the confluence area. Up to these latitudes, the meridian resolution is reduced in the Cartesian projection, reducing the capability of the gridded products to accurately represents the mesoscale signal in high latitudes areas~~. The effects of this change are discussed in Appendix C. Note, however that the grid resolution does not correspond to the spatial scales of the features that are resolved by the DT2014 SLA field. These spatial scales are about the same (perhaps slightly smaller) than in the DT2010 fields; they are imposed by the spatial correlation function used in the OI mapping procedure. In a~~A~~ddition~~ally~~ to the grid standards change, the area defined by the global product was extended ~~up~~ towards the poles in order to take into account the high latitude sampling offered by the more recent altimeters such as~~like~~ C2 (i.e. up to ±88°N).

Another important change implemented in DT2014 is the use of ~~better~~ more accurately defined correlation scales for~~of~~ the signal we want to map, and a more precise estimation of the error~~s~~ budgets associated with the different altimeter measurements. These two parameters indeed have a direct impact on~~for~~ mapping improvements as ~~underlined~~ underscored by previous studies (Fieguth et al, 1998; Ducet et al 2000; Leben et al 2002; Griffin et al, 2012, among others). The spatial variability of the spatial and temporal scales of the signal (see Dibarboure et al., 2011) is better accounted for~~taken into account~~. Both the spatial and temporal scales are defined as ~~a~~ functions of latitude and longitude. The spatial correlation scales however stay mainly depende~~a~~nt on~~f~~ latitude. The zonal (meridional) correlation scales range between 80 (80) km and ~400 (300) km. The larger values are observed in the low latitude band (±15°N) where they are mainly representative of the equatorial wave signature. At mid-~~-~~latitudes (between 20° and 60°), a global reduction of the correlation scales is observed in the poleward direction. The typical values observed range between 100(100) km and 200(150) km for zonal (meriodional) scales. Poleward of~~from~~ 60°, local increases up to 200 km of the correlation can be observed. Temporal scales are more depende~~a~~nt on~~f~~ both longitude and latitude position. Shorter temporal scales are fixed at~~to~~ 10 days. The longer scales are observed at mid latitudes (20 to 60°) where maximum observed~~al~~ values ~~observed~~ range between 30 and 45 days. Propagation speeds are also taken into account. They are mainly westward oriented with extreme values ranging to nearly 30 cm ~~.~~s^{-1} for latitudes around 5° to a few cm ~~.~~s^{-1} at~~in~~ high latitudes. Eastward propagations of a few cm ~~.~~s^{-1} are also observed close to the equator and in the circumpolar jet.

O~~The o~~bservation errors are defined with an uncorrelated component and an along-track long-wavelength correlated component (see Appendix B). The variance of the uncorrelated errors is defined assuming an ~~initial~~ 1 Hz initial measurement noise of nearly 3 cm for Topex/Poseidon, Jason-1, Jason-2 and AltiKa. Nearly 4 cm is used for the other~~s~~ altimeters. The effect of the filtering and sub-sampling that is applied to~~on~~ the measurement is taken into account and modulates the initial noise estimation. In addition to this noise effect, nearly 15% of the signal variance is used to take ~~into~~ account of~~the~~ small scale variability, which cannot be retrieved (see discussion in Le Traon et al., 2001). A~~The a~~dditional errors induced by the geodetic characteristics of some orbits (and also the use of a gridded MSS, rather than a more precise MP, as explained above~~here before~~) are taken into account. In the same way, ~~we also included~~ additional ~~errors~~variance i~~w~~as included in the altimeter error budget ~~of for the altimeters~~ for which the absence of dual-frequency and/or radiometer measurements leads to the necessity for a~~to use~~ model correction for the ionospheric and dry-troposphere signal corrections. The variance associated with along-track long-wavelength correlated errors corresponds to the residual orbit errors, as well as tidal and dynamic atmospheric signal correction errors. In the DT2014 products, the long-wavelength residual ionosphere signal, that can be observed when this correction is obtained~~deduced~~ from a model (typically for missions with mono-frequency measurements), is taken into account for ERS-2, C2 and HY-2A. In the same way, geodetic missions, for which no precise mean profile is available (see Sect. ~~hereafter~~*“Along-track SLA generation”*), present additional long-wavelength errors induced by the use of a global gridded Mean Sea Surface for the SLA computation. These ~~MSS~~ additional MSS errors a~~we~~re taken into account in the reprocessed products for C2, J1 geodetic phase, EN on it geodetic orbit and HY-2A. In~~At~~ the end, the variance of long-wavelength errors represents between 1 to 2% of the signal variance in high variability areas (e.g., the Gulf Stream, Kuroshio, …) and up to 40% in low variability areas~~,~~ and in high ionospheric signal areas for missions without dual-frequency measurement.

As previously stated, two gridded SLA products are computed, using two different altimeter constellations. The all-sat-merged products take advantage of all the altimeter measurements available. This allows an improved signal sampling when more than 2 altimeters are available (Fig. 1). The mesoscale signal is indeed ~~better~~ more accurately reconstructed during these periods (Pascual and al, 2006), when omission errors are reduced by the altimeter sampling. In the same way, high latitude~~s~~ areas can be better sampled by at least one of the available altimeters~~ available~~. These products are however not homogeneous in time, leading to interannual variability of the signal that directly linked to~~with~~ the evolution of the altimeter sampling. In order to avoid this phenomenon, ~~the ~~two-sat -merged products are also made available~~delivered~~. These are a~~y~~ merging of data from~~e~~ two altimeters following the TP and ERS-2 tracks (e.g., TP, then J1 then J2 merged with ERS-1 then ERS-2 then EN then AL (or C2 when neither EN nor AL are available)) in order to preserve,~~secure~~ as much as possible, the temporal homogeneity of the products. Excepting for the differences in~~of~~ altimeter constellations, the mapping parameters are the same for the all-sat-merged and two-sat-merged products.

Derived product~~s~~ generation:

Derived products are also disseminated to the users. These~~y~~ consist of the~~in~~ Absolute Dynamic Topography (ADT) (maps and along-track) and maps of geostrophic currents (absolute and anomalies).

The ADT products are obtained by adding a Mean Dynamic Topography~~ie~~ (MDT) to the SLA field. The MDT used in the DUACS reprocessing is the MDT CNES/CLS 2013 (Mulet et al, 2013), corrected to be consistent with the 20-year reference period used for the SLA.

The geostrophic current~~s~~ products disseminated to ~~the ~~users are computed using a~~the~~ 9-point stencil width methodology (Arbic et al, 2012)~~,~~ for latitudes outside the ±5°N band. Compared with the historical centered difference methodology, the stencil width methodology allows us to correct the anisotropy inherent~~inerrant~~ to the Cartesian projection. It also leads to slightly higher current intensities~~y of the current~~. In the equatorial band, the Lagerloef methodology is used, with various improvements compared to the previous DUACS 2010 version. Indeed, the meridional~~an~~ velocities are introduced into the β component. Moreover, ~~the ~~filtering of the β component~~s~~ is reduced, leading to more intense currents and improving the continuity of the currents within~~at~~ the latitudes ±5°N. The reader should~~must~~ however note that this paper is focused towards a~~s on~~ quality description of the SLA products~~ quality description~~. With this objective, the geostrophic currents used for~~in~~ different diagnostics presented within this~~the~~ paper are~~were~~ obtained using the same methodology (centered differences) for DT2014 and DT2010 datasets (see also Sect. 2.3.1).

Product~~s~~ format and nomenclature:

The DT2014 SLA products and derived products are distributed in ~~a~~ NetCDF-3CF format convention ~~and~~ with a new nomenclature for files and directory~~ies~~ naming~~es~~. Details are given in the user handbook (~~AVISO~~Aviso/DUACS, 2014b).

1.1.1 Reference period and SLA reference convention

Due to ~~the~~ incomplete~~poor~~ knowledge of the g~~G~~eoid at small scales and to ease the use of the altimeter DUACS products, the altimeter measurements are co-located onto theoretical tracks and a time average is removed (Dibarboure et al 2011, Sect 2.2.1). Consequently, the sea level anomalies provided in the L3 and L4 DUACS products are representative of variations of the sea level relative to the given period, called the altimeter reference period. Since 2001, the SLA~~y~~ have been referenced to a 7-year period [1993, 1999]. In 2014, with more than 20 years of altimeter measurements available, it was of high interest to extend the altimeter reference period to 20 years [1993-2012].

Changing from a 7 to 20 year~~s~~ reference period leads to ~~obtain~~ more realistic oceanic anomalies, in particular at~~the~~ interannual and climate scales. Indeed, t~~T~~he change of reference period from 7 ~~years~~ to 20 years not only integrates the evolution of the sea level in terms of trends, but also in terms of interannual signals at small and large scales (e.g., El Niño/Niña) over~~in~~ the 13 last years. Fig. ~~6~~ 5 (b) shows an example of this impact on a specific track from~~of~~ J2 over the Kuroshio region. It clearly ~~underlines~~ underscores the~~a~~ different SLA signature of the amplitude of the stream. The reference period change from 7 ~~years~~ to 20 years~~,~~ induces ~~the~~ global and regional Mean Sea Level (MSL) variations, as~~and is~~ plotted in Fig. ~~6~~ 5 (a)~~. The figureIt represents the change that users will observe in the DT2014 version of the product compared to DT2010~~. It also includes the adjustment of the SLA bias convention. The latter~~It~~ consists of having a mean SLA null over the year 1993. The use of this convention for the SLA leads to the introduction of an SLA bias between the DT2014 products and the former version. In Delayed time, this bias is estimated to be~~at~~ nearly 0.6 cm. The Fig. 5(a) represents the change that users will observe in the DT2014 version of the product compared to DT2010

The altimeter reference period change also impacts the Mean Dynamic Topography (MDT) field. Indeed, as long as the MDT is combined with the SLA in order to estimate the Absolute Dynamic Topography (ADT), the reference period the MDT refers to must be coherent with the reference period that the SLA refers to. The latest~~last~~ MDT_CNES_CLS13 (Rio et al, 2010) available from~~on~~ ~~AVISO~~Aviso is based~~distributed~~ on a 20-year reference period, consistent with the DT2014 SLA ~~DT2014~~ products.

The ~~Annex~~ Appendix A gives an overview of the relationship between SLA and MDT over different reference periods.

~~1.1.2 L3 Along-track noise filtering~~

~~As explained in the Sect. 2.2.1, the gridded products processing parameters is a trade-off between the altimeter constellation sampling capability and signal to retrieve. For DT2010, the processing, and in particular the along track noise filtering was set up in accordance to this objective. Consequently, the global DT2010 along-track SLA products were so far low-pass filtered with lanczos cut-off lengths depending on latitude (250km near Equator, until 55km at high latitudes). This technical choice was mostly linked to the ability of the TP altimeter mission to capture ocean dynamics mesoscale structures (Le Traon and Dibarboure 1999). However it reduced strongly the along-track resolution that might be useful and beneficial to modeling and forecasting systems. That is why a dedicated along track product, preserving the along track 1Hz high resolution signals has been developed in the frame of the DT2014 reprocessing. The main inputs come from the Dufau et al study (2014).~~

~~This study is based on spectral analysis, where the minimum length scale reachable with along-track altimeter data is determined as the point where signal and error are of the same order of magnitude. The mesoscale capability average over the World Ocean is 55km but appears lower in the equatorial band (20°S-20°N) and in the Western Boundaries Currents. The small-scale capability prescribed by this method at low latitudes being partly due to the limit of the underlying Surface Quasi Geostrophy turbulence in these areas, this region is retrieved. The mean mesoscale capability used as the cut-off length for low-pass filtering is consequently 65km.~~

1.2 DT2014 gridded SLA product~~s~~ validation protocol

C~~The c~~omparisons between the DT2014 and DT2010 products, as well as ~~the~~ comparison between altimeter gridded products and independent measurements, are presented in ~~section~~ Sect. 3. In this section we present the methodology used to assess the DT2014 SLA gridded products version and compare it with the DT2010 version. ~~Here w~~We ~~discuss in the section the methodology on comparison of the different products.~~

1.2.1 Altimeter gridded product~~s~~ intercomparison

The DT2014 and DT2010 SLA gridded products were compared over their~~y~~ common period [1993, 2012]. The DT2010 products were first processed in order to ~~homogenize~~ ensure~~make~~ consistency~~t~~ in~~the~~ resolution and physical content. In this way,

- The DT2010 products considered correspond to the ¼°x1/4° Cartesian resolution products previously identified as “QD” products. These products were obtained~~deduced~~ from the native DT2010 ~~original~~ grid layout~~resolution~~ (1/3°x1/3° Mercator grid, see Sect. 2.2.1~~2.2.1~~) using~~by~~ bi~~-~~linear interpolation.
- The DT2010 SLA was referenced to the 20-year altimeter reference period (see Sect. 2.2.2~~2.2.2~~). The reader should~~must~~ note that this reference change is not applied when working on ADT fields since ADT is not ~~impacted~~ affected by the altimeter reference period as explained in ~~Annex~~Appendix A.

In order to asse~~ce~~ss ~~the~~ SLA gradient~~s~~ quality, t~~T~~he geostrophic currents and derived EKE were also compared. G~~In this order, g~~eostrophic currents were computed using the same methodology (~~here~~ centered differences) for both the~~on~~ DT2010 and DT2014 products.

1.2.2 Comparison between gridded products and independent along-track measurements

The quality of the gridded ~~products~~ SLA field ~~quality~~ is estimated by comparing SLA maps with independent along-track measurements. Maps produced by merging of only two altimeters (i.e., “two-sat-merged” products; see Sect. 2.2.1) are compared with SLA measured along the tracks from~~following~~ other obits. This comparison is possible only when three or four altimeters are available. In this way, TP tandem (TPN) is compared with a gridded product that merges~~ing~~ J1 and EN over the years 2003-2004. The SLA is filtered in order to compare wavelengths ranging between 65-500 km that ~~,~~ characterize~~ing~~ medium and large mesoscale signals. The smallest scales (less than 65 km) are excluded in order to reduce the ~~impact~~ signature of along-track random errors (see Sect. 2.2.1 “*Along-track SLA generation*”~~2.2.3~~). The variance of the SLA differences between gridded ~~product~~ SLA fields and along-track SLA measurements is analyzed over different spatial selections. The same comparison is done using the previous DT2010 version of the products (processed as described in section 2.3.1) in order to estimate the improved accuracy of the new DT2014 ~~products~~gridded SLA fields. We assume as a first approximation that the errors observed in~~on~~ along-track products at these wavelengths is lower than~~t~~ the errors of the gridded products. Indeed, map~~ping~~ processing leads to ~~the~~ smoothing/loss~~missing~~ of the small scale~~s~~ signals, as previously discussed, and the random noise signals observed in the~~on~~ along-track products is minimized by the applied filtering ~~applied~~. The variance of the differences between gridded~~s~~ and along-track products thus mainly ~~traduces~~ expresses the imprecision of mesoscale~~s~~ reconstruction in~~with~~ gridded products. This is, however, a strong approximation since it does~~id~~ not consider correlated errors between ~~both~~ the two datasets (the altimeter standards used are quite homogeneous from one~~an~~ altimeter to the other, see Sect. 2.1).

1.2.3 Comparison between gridded products and in-situ measurements

Different in-situ measurements were used during the validation of the altimeter gridded products. ~~We present in~~ In this section we present the methodology used for the different in-situ comparisons.

Tide gauges:

Monthly mean t~~T~~ide g~~G~~auge~~s~~ (TG) data ~~(TGs)~~ from the PSMSL (Permanent Service for Mean Sea Level) database with a long life~~-~~times (> 4 years) were used. The TG data processing is described by Valladeau et al (2012) and Prandi et al. (2015). The Sea Surface Height measured by the TGs is compared to the monthly mean SLA field given by altimeter gridded products merging all the altimeters available (i.e. “all-sat-merged” products). As described by Valladeau et al (2012) and Prandi et al. (2015), data collocation is based on a maximum~~al~~ correlation criterion.

Temperature/s~~S~~alinity profiles:

Quality controlled Temperature/Salinity (T/S) profiles from the ~~Coriolis~~ CORIOLIS Global Data Assembly Center were used. The T/S profiles processing used in this paper is the same as described by Valladeau et al (2012) and Legeais et al (~~2015~~2016). The Dynamic Height Anomalies (DHA) deduced from T/S profiles (reference depth 900 dbar) are ~~them~~ compared to the ~~equivalent~~ SLA fields ~~deduced~~ from gridded "all-sat-merged" ~~SLA~~ products. As discussed by~~in~~ Legeais et al (2016), the DHA are representative of the steric effect above the reference depth, while SLA is representative of both barotropic and baroclinic effects affecting the entire water column. In spite of this difference of physical content, the relative comparison between altimeter SLA and in-situ DHA is sufficient to detect differences between two SLA altimeter products.

Surface drifters:

Surface drifters distributed by the AOML (Atlantic Oceanographic & Meteorological Laboratory) over the period 1993-2011 were processed in order to extract the absolute geostrophic component only. In this way, they were corrected for the~~from~~ Ekman component using the model described by Rio et al. (2011). Drifter~~s'~~ drogue loss was detected and corrected using the methodology described by Rio et al.~~,~~ (2012). A low-pass 3-day filter~~ing~~ is applied in order to reduce ~~the~~ inertial wave effects. Finally, the absolute geostrophic currents deduced from altimeter "all-sat-merged" SLA ~~maps~~ grids are interpolated to the~~on~~ drifter~~s~~ positions for comparison.

2 DT2014 products analysis

2.1 Mesoscale signals in the along-track products

The unique cut-off length of 65 km used for the along-track product~~s~~ low-pass filtering (see Sect. 2.2.1 "*Along-track SLA generation*"~~2.2.3~~) drastically changes the content of the SLA profiles, especially in low latitudes areas where wavelengths from nearly 250 km (near the equator) to 120 km (near ±30°N) were filtered in the DT2010 products. Higher resolution SLA profiles are now provided.

Spectral analysis applied to the~~on~~ new products confirms the~~that~~ addition of energy in the mesoscale dynamics band at low latitudes: The new along-track SLA preserves the energy of the unfiltered data ~~down tountil a~~for length scales greater than~~ of~~ 80 km in the equatorial band, and~~but~~ also in the mid latitudes high variability areas although the~~less~~ impact of the~~ed by this~~ filtering change is less. Fig. 4~~5~~ shows the variance of the short wavelength signal ~~filtered ~~removed (by low-pass filtering) from J2 along-track products over year 2012, both for~~in~~ DT2010 and DT2014. In the DT2010, the wavelength removed ranged between 250 to 65km, depending on the latitude. In the DT2014, only wavelength lower 65km were filtered. ~~versions.~~ The figure ~~underlines ~~shows an important variance in the mid~~dle~~ latitudes areas and equatorial regions. The variance~~It~~ is directly linked to the 1 Hz altimeter measurement error that is highly correlated with the significant wave height and inconsistency~~unhomogeneity~~ in the radar backscatter coefficient (Dibarboure et al, 2011~~4~~; Dufau et al, ~~2014~~2016, ~~in review~~). In the DT2010 dataset, the filtered wavelength signal ~~filtered ~~is clearly more important in the latitudes ranging between ±~~+ ~~40°N, underlining part of the physical signal~~.~~ that is also reduced by the filtering applied.

2.2 Mesoscale signals in the gridded products

2.2.1 Additional signal observed in DT2014 compared to DT2010

The mapping process optimization (see Sect. ~~-~~2.2.1) directly ~~impacts ~~affects the SLA physical content observed within the gridded products. The differences between DT2014 and DT2010 temporal variability of the signal for the period [1993, 2012] are~~is~~ shown in Fig. ~~7 ~~6 ("all-sat-merged" product). The figure~~It~~ ~~underlines ~~shows additional variability in the DT2014 products. The global mean SLA variance is now increased by nearly +3.5 cm² within the latitude~~s~~ band ±60°N. T~~H~~his~~It~~ represents 5.1% of the variance of the DT2010 "QD" products. This increase is mainly due to the mapping parameters including two main changes in the DT2014 products. The first one, that explains +3.6% of the variance increase, is the change of the native grid resolution. ~~TIndeed, the~~ DT2014 was ~~directly~~ computed directly on the 1/4°x1/4° Cartesian grid resolution (see Sect. 2.2.1~~2.2.1~~), while the DT2010 "QD" product was interpolated linearly~~considered was not directly computed~~ at~~on this grid resolution, instead it was interpolated limearly but is deduced~~ from the ~~original~~ native 1/3°x1/3° Mercator resolution product~~ by linear interpolation~~ (see Sect. 2.3.1). This interpolation process~~ing~~ slightly smoothes the signal, and directly contributes to redu~~e~~ction of~~e~~ the variance of the signal observed in DT2010. The second change implemented in the DT2014 products is the use of improved correlation scales, associated with the change of the along-track low-pass filtering presented in ~~the~~ chapter 2.2.1 "*Multi-mission mapping*"). This change~~It~~ contributes to an increase in the SLA variance of~~by~~ +1.5%. Finally, additional measurements (e.g., C2 in 2011) that were not included in the DT2010 products also contribute to improvements in the signal sampling, and thus increase the variance of the gridded signal.

The additional signal observed in the DT2014 products is not uniformly distributed as ~~underlined~~ shown in Fig. ~~7~~6. Indeed, the main part of the variance increase (from +50 to more than +100 cm²) is observed in the higher variability areas and coastal areas. It ~~traduces~~ is an expression of~~es~~ the ~~better~~ more accurate reconstruction of the mesoscale signal in the DT2014 products, as discussed below~~after~~. In some parts of the o~~O~~cean we however observe a decrease~~ing~~ of the SLA variance. The improved standards used (see Sect.~~–~~ 2.1) indeed contribute to local~~ly~~ reductions of~~e~~ the SLA error variance. The main reduction is observed in the Indonesian area with ~~and~~ amplitudes ranging 2 to 3 cm². The SLA error variance is also reduced in the Antarctic area (latitudes < 60°) with the ~~locally~~ higher local amplitudes. The improved DAC correction using ERA-Interim reanalysis fields over the first decade of the altimeter period is a~~,~~ significant~~largely~~ contributor~~es~~ to the variance reduction (Carrere et al., 2015).

A~~The a~~nalysis of the spectral content of the gridded products over the Gulf Stream area (Fig. ~~9~~8) shows that all of the DT2014 products are impacted at small scales, i.e., wavelengths lower than 250-200 km. For "all-sat-merged" as well as "two-sat-merged" products the energy observed in ~~the~~ DT2014 for wavelengths around 100 km ~~are~~ is twice as high as that~~e~~ ~~one~~ observed ~~twice more important in the DT2014 than~~ in the DT2010 ~~maps~~gridded SLA products, both in the zonal and meridian directions. The maximum additional signal is observed for wavelengths ranging between 80-100 km. For these wavelengths, the DT2014 products have 2 to 4 times more energy than ~~in~~ the DT2010 versions. Nevertheless, the energy associated with~~to~~ these wavelengths -falls drastically for- ~~fall~~ both ~~for~~ DT2014 and DT2010 SLA products, meaning that DT2014 still misses a large part of the dynamic signal at these wavelengths, as discussed in Sect. 4. ~~. These wavelengths are considered as the minimal scales fully observable with conventional altimetry, especially with a two-altimeter constellation (Pascual et al, 2006, Pujol et al. 2005), and thus all the more difficult to interpolate in a 2D grid, at least with conventional mapping method (Escudier et al, 2013; Dussurget et al, 2011). Moreover, the spatial grid resolutions used for DT2010 and DT2014 products, as well as the parameters used for the map construction (e.g. correlation scales), are not adapted for resolving scales smallest than 100 80 km. The energy associated to these wavelengths drastically fall both for DT2014 and DT2010 products.~~

Compared to the DT2010 products, the new DT2014 version has~~presents~~ more intense geostrophic currents (see Sect. 2.3.3). This has a direct ~~impact~~ signature on the eddy kinetic energy (EKE) that can be estimated from the two different versions of the product. ~~The~~ Figure~~.~~ ~~10~~ 9 shows the spatial differences of the mean EKE computed~~deduced~~ from the DT2014 and DT2010 products as described in section 2.3.1. As previously observed ~~on~~ with the SLA variance, the EKE is higher in the DT2014 products. An a~~A~~dditional 400 cm^2/s^2 in levels of EKE are observed in the DT2014 products in high variability areas. This represents a 20% EKE increase compared to ~~the~~ DT2010.~~is more important in the DT2014 products, especially in high variability areas where belong +400~~ ~~cm^2/s^2~~ ~~are observed. This however represents less than 20% of the DT2010 signal.~~ Proportionally, the EKE increase observed in~~with~~ the DT2014 products is quite important in low variability areas and Eastern boundary coastal currents where it ~~can represent below~~ reaches up to 80% of the DT2010 EKE signal, as ~~underlined~~ underscored by Capet et al (2014). The global mean EKE increase, excluding the equatorial band and high latitude~~s~~ areas (> ±60~~5~~°N), represents nearly 15% of the ~~energy~~ EKE observed in the DT2010 products. This additional energy is induced by different changes implemented in the DT2014 products (see Sect. 2.2.1). Nearly 10% of the additional energy is associated with the signature of the ~~direct computation~~interpolation from~~of~~ the native DT2010 SLA 1/3°x1/3° Mercator grid onto the 1/4°x1/4° Cartesian grid ~~for DT2014~~ (see Sect. 2.3.1). The improved mapping parameters, especially the change of ~~the~~ correlation scales and reduced along-track filtering used in the DT2014 ~~products~~gridded SLA field construction, leads to~~induce~~ an energy increase ~~of the energy~~ of nearly +6%.

2.2.2 Impact of the altimeter reference period on EKE

~~The~~ Figure~~.~~ ~~11~~ 10 shows the temporal evolution of the m~~M~~ean EKE over the global ocean both for DT2014 and DT2010. We first note the nearly 15% additional mean EKE i~~o~~n the DT2014 product as previously discussed. We also note a significant difference in~~of~~ the EKE trend between DT2014 and DT2010, where~~n~~ the latter is ~~kept~~ on the 7-year altimeter reference period (Sect. 2.2.2). Indeed, the mean EKE trend is nearly -0.0265 (-0.45) cm^2s^{-2}/year when DT2010_ref7y (DT2014) products are considered. On the other hand~~At the opposite~~, when DT2010 is referenced to the 20-year period, the EKE trend (-0.369 cm^2s^{-2}/year) is comparable to the DT2014 (-0.45 cm^2s^{-2}/year). This result clearly ~~underlines~~ emphasizes the sensitivity of the EKE trend estimation to the altimeter reference period~~ used~~. Indeed, the use of the 20-year reference period leads to a minimized signature of the SLA signal over this period. Conversely~~At the opposite~~, the SLA gradients are artificially higher after ~~year~~ 1999 when the historical [1993, 1999] reference period is used. As a consequence~~s~~, after ~~year~~ 1999, the EKE ~~deduced~~ from the DT2010 products (~~let~~ on the 7-year reference period) is higher than the EKE ~~deduced~~ from the DT2014 products (we do not consider here the global mean EKE bias observed between the two products).

2.2.3 DT2014 gridded product~~s~~ error~~s~~ estimates~~ion~~ at the mesoscale~~s~~ and error~~s~~ reduction compared to DT2010

The accuracy of the gridded SLA products is estimated through~~by~~ comparison with independent along-track products, focusing on mesoscale signals, as described in section 2.3.2. The results of the comparison between gridded and along-track products are shown in Fig. 11~~12~~ and summarized in~~on~~ Tab. 1.

The gridded product~~s~~ errors for~~on~~ mesoscale~~s~~ wavelengths usually range between 4.9 (low variability areas) and 32.5 cm^2 (high variability areas)~~,~~ when excluding coastal and high latitude~~s~~ areas. They can, however, be lower, especially over~~on~~ very low variability areas such as ~~in~~ the South Atlantic Subt~~-T~~ropical gyre (hereafter “reference area”) where the observed errors ~~observed reach~~are nearly 1.4 cm². It is important to note that these results ~~underline~~ are representative of the quality of the “two-sat-merged” gridded products. These~~It~~ can be considered to be~~as a~~ degraded products for ~~the~~ mesoscale mapping since they use~~ing a~~ minimal altimeter sampling. On the other hand~~At the opposite,~~ the “all-sat-merged” products, during the periods when three or four altimeters were available, benefit~~s~~ ~~form~~ from ~~an~~ improved surface sampling. ~~-~~The errors in~~on~~ these products should thus be lower than those observed in~~on~~ the products that merge~~ing~~ only two altimeters.

Compared to the previous version of the products, the gridded ~~products~~ SLA errors are reduced. Far from the coast, and for ocean variances lower than 200 cm², the processing/parameter~~s~~ changes included in the DT2014 version lead to a reduction of ~~nearly~~ 2.1% of the variance of the differences between gridded products and along-track measurements observed with DT2010. The reduction is higher when considering high variability areas (> 200 cm²), where the impact of the new DT2014 processing is maximum. In this~~that~~ case, it reaches ~~nearly -10~~9.9%. On the other hand~~At the opposite~~, some slight degradation is observed in ~~the~~ tropical areas, especially in the Indian Ocean. In that region, up to 1 cm² increased variance of the differences between grids and along-track estimates is observed. This can be~~is~~ directly linked to~~with~~ the change of the processing in these latitudes, especially the reduction of the short wavelength filtering applied before the mapping process, as explained in Sect. 2.2.1.

2.2.4 DT2014 g~~G~~eostrophic current~~s~~ quality

The improved mesoscale~~s~~ mapping also ~~impacts~~ affects the quality of the geostrophic current estimation~~ed~~, which is directly linked to ~~the~~ SLA gradients. Geostrophic currents computed~~deduced~~ from ADT altimeter gridded products were compared with geostrophic currents measured by drifters. The altimeter and drifter product~~s~~ processing procedures are summarized in sections 2.3.1 and 2.3.3.

The distribution of the ~~intensity~~ speed of the current (not shown), ~~underlines~~ shows a global underestimation of the current in the altimeter products compared to the drifter~~s~~ observations, especially for currents with medium~~an~~ and strong intensities~~y~~ (> 0.2 m/s). However, in both ~~the~~ cases, the DT2014 current~~s~~ ~~intensity~~ speeds are~~is~~ still closer to the drifter distribution. The ~~variability~~ rms of the zonal and meridional components of the currents ~~is~~ are also increased in the DT2014 dataset and hence~~to be~~ closer to the observations. ~~The~~ Taylor skill~~s~~ scores (Taylor, 2001), that take~~s~~ into account both correlation and ~~variability~~ rms of the signal, are~~is~~ given in Tab. 2. Outside the equatorial band, the Taylor score is 0.83 (0.83) for the zonal (meridional~~an~~) component. Compared to the DT2010 products, this ~~it~~ is an increase of~~d by~~ 0.01 (0.02).

V~~The v~~ariance reduction of the differences between altimetry and drifter~~s~~ zonal and meridian components is shown in Fig. 12~~13~~. C~~The c~~ollocated comparisons of zonal and meridional~~an~~ components show that this improvement is not consistent~~homogeneous~~ in space, and that errors in the position and shape of the structures mapped by~~from~~ altimeter measurements are still observed in the DT2014 products. Outside the equatorial regions (±10°N), the variance reduction observed with the DT2014 product is nearly -2.1 (-1.2) cm²/s², i.e., -0.55 (-0.34)% of the drifter variance for the zonal (~~meridian~~meridional) component. Locally, this reduction can reach more than -10%. Such~~It~~ is the case, for instance, in the Gu~~o~~lf of Mexico and tropical Atlantic Ocean. In contrast~~At the opposite~~, local degradation (ranging from 2 to 15% of the drifter variance) is observed within the tropics. The degradation is especially significant in the Pacific (z~~Z~~onal component), North Indian Ocean, and n~~N~~orth of Madagascar. These areas correspond quite well ~~correspond~~ with regions with high amplitudes of the M2 internal tide that are still present in the altimeter measurements and affect the non-tidal signal at wavelengths near~~ly~~ 140 km (Dufau et al, ~~2015~~2016). The degradation of the current seems to ~~underline~~ underscore a noise-like signal in the SLA gridded products. This~~It~~ could correspond to the signature of the~~is~~ tidal signal, which more prominent~~important~~ in the DT2014 ~~version~~ gridded products as ~~underlined~~ shown by Ray et al (2015). This is certainly reinforced by reduced filtering and the smaller temporal/spatial correlation scales used in this version (Sect. 2.2.1).

2.3 Coastal areas and h~~H~~igh l~~L~~atitudes

As described in Sect. 2.2.1, processing in~~the~~ coastal regions ~~processing~~ has also been improved. The most visible ~~impact~~ change is the increased ~~grids~~ spatial coverage of the grid in coastal areas ~~greatly improved~~. The DT2014 grid more closely approximatess ~~indeed better fit with~~ the coastline, as illustrated in Fig. 7~~8~~ (c, d). This is achieved~~induced~~ both by ~~the~~ tuning of the grid definition near the coast, and by the improved definition of the MPs close to the coast (see Sect. 2.2.1) that allow~~ing~~ improved data availability in these~~is~~ nearshore areas.

S~~The grids s~~patial grid coverage is also greatly improved i~~I~~n the Arctic region, as illustrated in Fig. ~~8~~ 7 (a, b). As above~~previously~~, the tuning of the SLA mapping parameters and availability of MPs in this region directly contribute~~leads~~ to this result. Additionally, the reduced errors that contribute to reduction of the SLA variance as shown in Fig. ~~7~~6, are also a result of ~~induced by~~ a more finely tuned ~~thinner~~ data selection process ~~tuned more finely~~ and ~~a~~ the more precise MPs (along ERS-1/2 and EN tracks) used in the DT2014 product (see Sect. 2.2.1~~2.2.1~~) ~~contribute to reduce the SLA variability variance as underlined shown on Fig. 76~~. In the Laptev Sea, a strong local ~~and strong~~ reduction (up to 100 cm²) of the SLA variance is observed. This~~It~~ is directly linked to~~with~~ the quality of the MP ~~used~~ (along ERS-1/2 and EN tracks), and also with the improved data selection (see Sect. 2.2.1), especially for geodetic missions (here mainly C2, and~~en~~ EN after its orbit change) for which precise MPs cannot be used.

The quality of the gridded SLA products near the coast (0-200 km ~~to the coast~~) was estimated by comparison with independent along-track measurements as explained in Sect. 2.3.2. Results are shown in Fig. ~~12~~ 11 and Tab. 1. The mean error variance reaches 8.9 cm². It can be more important in areas of high coastal variability ~~areas~~, where up to more than 30 cm² can be observed (Indonesian/Philippi~~a~~nes coasts, Eastern Australian coasts, North~~ern~~ Sea coasts and coasts located in~~at~~ proximity to the w~~W~~estern boundary currents~~streams~~). The DT2014 processing resulted in~~induced~~ a global reduction of these differences compared to the DT2010 products. They~~It~~ reache~~s~~ 4.1% of the error variance observed in the~~on~~ DT2010 products. However, local degradations are observed, such as along the Philippine~~ans~~ coasts.

The comparison between gridded SLA products ~~–~~(merging of all the available altimeters ~~available~~) and monthly TG measurements (see Sect. 2.3.3 for methodology) also ~~underlines~~ emphasizes a global improvement in~~of~~ the DT2014 products in ~~the~~ coastal areas. The variance of the differences between sea level observed with DT2014 ~~altimeter DT2014~~ gridded ~~products~~ altimetric SLA fields and TG measurements is compared with the results obtained using the DT2010 gridded ~~products~~SLA fields. The results (Fig. ~~14~~13) show a global reduction of the variance of the differences between altimetry and TGs when DT2014 products are used. This reduction is quite clear at~~in~~ the n~~N~~orthern coast of the Gulf of Mexico, along the ~~Indian~~ e~~E~~astern Indian coasts, and along the US coasts (reduction of up to 5 cm², i.e., ~~form~~ from 2 and up to 10% of the TG signal). The Western Australian sea level is also ~~better~~more accurately represented in the DT2014 products (reduction of up to 2.5 cm², i.e., 1 to 2% of the TG~~s~~ signal). In contrast~~At the opposite~~, a local degradation of the comparison between altimetry and TGs is observed in the n~~N~~orth Australian and Indonesian area (increase~~augmentation~~ of up to 2 cm², with local values reaching up to 5 cm²)~~,~~ where it ~~however~~ represents, however, less than 4% of the TG~~s~~ signal. The local improvements seen via~~with~~ TG~~s~~ results are consistent with the conclusions from other diagnose~~i~~s, such as the comparisons between SLA grids and independent along-track measurements over~~in~~ the same coastal areas. ~~which thus reinforce our confidence in these good results.~~

2.4 Climate scales

Different processing and altimeter standards changes were defined in accordance with the SL_cci project (Sect. 2.1), and thus also have an impact on ~~the~~ MSL trend estimation, especially at regional scales.

The Global MSL trend measured with the DT2014 gridded SLA products over the [1993, 2012] period is 2.94 mm/year (no glacial isostatic adjustment~~GIA~~ applied). The comparison between DT2014 and DT2010 products (Fig. ~~15~~14, b) does not exhibit any ~~differences~~ statistically relevant differences. Although~~,~~ no impact is detected on the Global MSL trend, differences are observed at inter-annual scales (1-5 years). The main improvement is the ERS-1 calibration during its geodetic phase (i.e., from April 1994 to March 1995). The nearly 3 mm/year differences observed between DT2010 and DT2014 during this period ~~traduce~~ show an improvement in the DT2014 products. Indeed, a nearly 6 mm bias between ERS-1 and TP was~~were~~ observed in the DT2010 product and this was not entirely reduced when merging both of the altimeter measurements. This was corrected in the DT2014 version. Fig. 14~~15~~ (b) also ~~underlines~~ shows a global 5.5 mm mean bias difference between the mean SLA ~~form~~ from DT2014 and DT2010. This bias is directly linked to the global SLA reference convention used in the DT2014 version, as explained in Sect. 2.2.2.

The regional MSL trend differences between DT2014 and DT2010 (Fig. 14~~15~~, a) are similar to the differences ~~underlined~~ shown by Philipps et al, (2013a and 2013b) and Ablain et al (2015) between the SL_cci and DT2010 products (see fig 6 of the paper). As explained by the authors, the change of ~~the~~ orbit standards solution mainly explains the e~~E~~ast/w~~W~~est dipole differences.

In order to highlight the improved ~~regional~~ MSL trend estimation between the e~~E~~astern and w~~W~~estern hemispheres with the DT2014 product ~~at such hemispheric scales~~, the trend computed~~deduced~~ from the altimeter products was~~were~~ compared to the trend computed~~deduced~~ from in-situ T/S profiles (see Sect. 2.3.3 for processing). This comparison was done during the [2005, 2012] period when a significant number of in-situ measurements are available. One would~~should~~ expect ~~homogeneous~~ consistent differences between altimeter and in-situ measurements in both hemispheres. This~~It~~ is the case for the DT2014 products for which the MSL trend differences reach nearly 1.56 (1.68) mm/year in the e~~E~~astern (w~~W~~estern) hemisphere. Conversely~~AtIn the opposite~~, an ~~unhomogeneity~~ inconsistency can be~~is~~ observed with DT2010 since the MSL trend differences with in-situ measurements are 2.02 (1.05) mm/year, ~~underlining~~ showing the nearly 1 mm MSL trend differences between the~~both~~ hemispheres.

As ~~underlined~~ presented by~~in~~ Ablain et al (2015), the regional MSL trend comparison also show differences at smaller scales. Here again, the change of ~~some~~ standards is~~are~~ directly responsible for these differences. The use of the ERA-Interim reanalysis meteorological fields in the DAC solution (see Sect.2.1) mainly ~~impact~~ affects the regional MSL trend estimation in the southern high latitude~~s~~ areas, as ~~underlined~~ underscored by Carrere et al. (2015). The same meteorological forcing used in the wet troposphere correction slightly contributes to the regional improvement of the MSL trend, especially for the first altimetry decade (Legeais et al 2014). A portion~~Part~~ of the smallest regional scale~~s~~ differences are also induced by the improved inter-calibration processing in the DT2014 products, ~~better~~ that more accurately take~~ing into~~ account of the regional biases from one~~a~~ reference mission to an~~the~~ other (see Sect. 2.2.1).

Some of the improvements implemented in the DT2014 version also impact the interannual signal reconstruction at regional scales. The more accurate estimation of the ~~LWE~~ long wavelength errors associated with~~to~~ the ionospheric signal correction (see Sect. 2.2.1) leads to a reduced signature of these errors in the products, especially during ~~the~~ periods of high solar activity. This~~It~~ was the case in 2000, when ERS-2 measurements were ~~is~~ not taken in~~done on a~~ dual-frequency mode~~, that~~ preventing us from mak~~estimat~~ing a precise ionospheric correction. A~~The a~~dditional long wavelength errors~~LWE~~ in the polar equatorial band, induced by the use of a less precise model solution, are taken into account in the DT2014 products. C~~The c~~omparisons of the regional mean SLA from ERS-2 measurements with TP (for which a precise ionospheric correction is available) over the year 2000 (Fig. ~~16~~15) ~~underlines~~ underscores~~s~~ a residual ionospheric signal that locally reaches 5 mm. The same comparison done with DT2010 products shows that this residual error was almost twice as high than~~as~~ in the DT2014 version ~~quite two time more stronger in this version~~ with a~~locally~~ more than 1 cm local bias between ERS-2 and TP measurements.

1 Discussions and Conclusions

M~~For the first time, m~~ore than 20 years of ~~altimeter~~ L3 and~~to~~ L4 altimeter SLA products have been~~were~~ entirely reprocessed and delivered as the DT2014 version. This reprocessing takes into account the ~~last~~ most up-to-date altimeter standards, and also includes important changes in~~of~~ different parameters/methods involved at each step of the processing. T~~At the end, t~~he

~~changes~~ implemented changes impact the SLA signals at different spatial and temporal scales, from large to mesoscales and from low to high frequencies~~y~~.

One ~~important~~ important~~impacting~~ change that will have an impact on~~for~~ users~~change~~ is the~~consists in~~ referencing of the SLA products to~~on~~ a new altimeter reference period, taking advantage of the 20 years of available measurements ~~available~~ and leading to a more realistic ~~signature of~~ interannual SLA record~~ interannual signal~~. The variability of the SLA, as well as the EKE deduced from SLA gradients is thus changed compared to the DT2010 dataset, especially after 1999. This change is visible in~~on~~ the mean EKE trend over the 20 year period;~~,~~ it was overestimated in DT2010. This result~~impact~~ suggests that previous estimate~~ion~~s of EKE trends from altimeter products (e.g., Pujol et al, 2005~~-~~; Hogg et al., 2015) should be reviewed, taking into account the altimeter reference period.

Other changes were implemented in the DT2014 processing. They consist of~~in~~ using up to date altimeter standards and geophysical corrections, reduced smoothing of the along-track data, and refined mapping parameters, including spatial and temporal correlation scale~~s~~ definitions and measurement errors. This paper focuses on the description of the impact of these changes on the SLA gridded fields, through~~using~~ comparisons with independent measurements.

The SLA variability of the DT2014 dataset is more energetic than ~~the~~ DT2010. The ~~variability~~ variance of the SLA~~ signal~~ is increased by 5.1% in the DT2014 products, implying~~underlining~~ additional signals for wavelengths lower than ~250 km. A global ~~EKE~~ 15% EKE increase (equatorial band excluded; latitudes > 60°N) is also observed with DT2014. This increase is higher in low variability and eastern coastal areas where it reaches up to 80%. The interpolation process that is applied to the ~~on~~ DT2010 SLA grids (see Sect. 2.3.1) ~~direct computation of the DT2014 products on the ¼°x1/4° Cartesian grid~~ explains nearly 2/3 of the variability/energy ~~increase~~decrease compared to the DT2014 signal. The other 1/3 is directly linked to~~with~~ the improved parameterization of the DT2014 mapping procedure~~ssing~~. In contrast~~Contrary~~ to the DT2010 reprocessing (Dibarboure et al, 2011), the ~~impact~~ effect of the new altimeter standards is moderate in comparison with the ~~impact~~ effect of the processing changes. The improved accuracy of the along-track signal that is a result of~~,~~

~~induced by~~ the use of more accurate altimeter standards (see Sect.2.1) should contribute to a reduction of~~e~~ the SLA error variance observed with gridded products. This~~It~~ was the case when comparing DT2010 with previous DT2007 gridded products (Dibarboure et al, 2011). The DT2010 products did not include significant changes in the mapping processing, and the reduction of the SLA error variance, more important in the Indonesian area, was mainly explained by the use of improved altimeter GDR-C standards. However, the amplitude of this error variance reduction is ~~quite~~ almost 10 times less important than the ~~impact~~ effect of the mapping procedures~~ssing~~ changes implemented in the DT2014 products.

The additional signal observed in DT2014 is the signature of ~~traduces~~ the improved SLA signal reconstruction, especially at mesoscales, as previously ~~underlined~~ demonstrated~~emphasized~~ by Capet et al (2014) in the e~~E~~astern boundary upwelling systems. The DT2014 SLA product~~s~~ quality was estimated at global scales using comparisons with independent measurements (altimetry and in-situ) which allowed us to establish a refined mesoscale~~s~~ error budget ~~given~~ for the merged gridded products. The DT2014 SLA product~~s~~ errors for the mesoscale~~s~~ signal in the open ocean is estimated to be between 1.~~5~~ 4 cm² in low variability areas, and up to 32.5~~3~~cm² in high variability areas where the altimeter sampling does not allow a full observation of the SLA variability. Compared to the previous version of the products, this error is reduced by a factor up to ~~10~~9.9% in high variability areas.

Globally, g~~The g~~eostrophic currents are ~~globally~~ slightly intensified in the DT2014 products, becoming closer to the surface drifter~~s~~ observations. The geostrophic current are, however,~~, is~~ still ~~globally~~ underestimated compared to the in-situ observations. Outside the tropical band, the variance of the differences between altimeter products and in-situ observations is reduced almost everywhere. This reduction can ~~locally reache~~reach more than~~s up to~~ 10% of the in-situ variance. In contrast~~At the opposite~~, geostrophic currents estimated with DT2014 products have a ~~is~~ globally lower correlation~~ed~~ with in-situ observations within the tropics. This degradation ~~locally~~ represents up to 15% of the in-situ variance.

DT2014 SLA products were also improved in coastal and high latitude areas. The main improvements are~~is~~ visible in~~on~~ the spatial coverage, refined in coastal areas and improved in Arctic regions with a ~~better~~ more precise definition of the coastline and sea ice edge. The

~~errors of~~ SLA gridded product errors in the coastal areas (< 200 km) are estimated at~~nearly~~ ~~9~~ 8.9 cm^2, with higher values in high variability coastal areas. This error is globally reduced by 4.1% compared to the previous version of the products. C~~The c~~onsistency with TG~~s~~ measurements is improved, especially in different areas such as the n~~N~~orthern coast of the Gulf of Mexico, along the Indian ea~~E~~astern coasts and along the US coasts. In this~~that~~ case the reduction of variance of the differences between altimetry and TGs ranges between 2 and up to 10 % of the TG~~s~~ signal, when compared to the results obtained with DT2010 products. In some other coastal areas, degradation is however ~~underlined~~observed. This~~It~~ is the case in the n~~N~~orth Australian and Indonesian areas where it reaches less than 4% of the TG~~s~~ signal.

The quality of the regional SLA products is not specifically addressed in this paper. However, as for the global products, mapping was also improved at regional scale with a positive impact in coastal areas, as ~~underlined~~ presented by Marcos et al (2015) and Juza et al (2015, under~~in~~ ~~preparation~~review) in the Mediterranean Sea.

~~Globally, the comparison to different independent measurements gives consistent results, highlighting improvement or degradation in the same areas, reinforcing our confidence in these results.~~

C~~The c~~limate scales are also improved with DT2014, taking advantage of the altimeter standards and processing defined in line~~consistency~~ with the SL_cci project. The global MSL trend estimation is nearly unchanged in the DT2014 products compared to ~~the~~ DT2010. However, significant improvements are ~~underlined~~ observed at regional scales, with a reduction of the ±1mm/year dipole error observed in ~~the~~ DT2010 between eastern and western ~~basin~~hemispheres. Additionally, the residual ionospheric errors, previously observed i~~o~~n altimeter measurements without dual-frequency, are reduced by up to 50% in the DT2014 products.

The assessment of the quality of the DT2014 SLA products at mesoscales ~~underlined~~ underlines~~score~~ the limits of the products.

First, the spectral content of the gridded ~~products~~ SLA fields clearly ~~underlines~~ shows that part of the small signal is missing in the gridded products. Although small wavelengths can be resolved with 1 Hz along-track products (up to nearly 80-100km~~lye~~ -in eastern basins where SLA signal to noise ratios limit~~s~~ ~~the~~ observations of ~~the~~ smaller wavelengths; satellite and seasonally dependent) (Dufau et al, 2016), the temporal and spatial across-track sampling of the dynamical structures at these wavelength is, however, limited and they are difficult to interpolate onto~~in~~ a 2D grid, especially with a two-altimeter constellation (Pascual et al, 2006, Pujol et al. 2005), and with conventional mapping methods (Escudier et al, 2013; Dussurget et al, 2011). The spatial grid resolutions used for the DT2010 and DT2014 products, as well as the parameters used for ~~the~~ maps~~s~~ construction (e.g., along-track low pass filtering, correlation scales, measurement errors) are a result of~~issued from~~ a compromise between the altimeter sampling capability and the physical scales of interest. They are not adapted to~~for~~ resolve~~ing~~ the small mesoscales. ~~Finally, the~~The resulting mean spatial resolution of the DT2014 global gridded ~~global products~~ SLA is comparable to the DT2010 resolution. It was estimated to be nearly 1.7°, i.e., ~~~150~~slightly less than 200 km at mid latitudes (Chelton et al, ~~2014~~2011, 2014). The comparison with the spectral content computed~~deduced~~ from full resolution AL 1Hz along-track measurements (not shown) ~~underlines~~ shows that nearly 60% of the energy observed in~~from~~ along-track measurements at~~on~~ wavelengths ranging from 200-65km is missing in the SLA gridded products~~21 cm² of the global ocean variance is missed with gridded products (wavelengths < 65km excluded; comparison with AL 1 Hz measurements over year 2013). It represents nearly 16% of the along-track signal and up to 40% when wavelengths ranging 300-65km are considered~~. In other words, nearly ~~2~~3/5 of the small-mesoscale variability is missing~~ed~~ in the~~with~~ DT2014 gridded products. This is clearly linked to the mapping methodology, combined with altimeter constellation sampling capability~~ies~~.

The second limitation of the DT2014 ~~product~~ gridded SLA fields is the additional non mesoscale signal that is observed. It is characteristic of the residual M2 internal tide, visible in~~on~~ both along-track (Dufau et al, ~~2015~~2016) and gridded products (Ray et al, 2015). The presence of this signal leads to local degradation of ~~the~~ DT2014 quality in specifics areas. The signature of ~~the~~ internal waves is on the same wavelengths as the~~than~~ mesoscale signal that the DUACS SLA products focus on, making ~~tricky the~~ reduction of this signal without affecting the mesoscale signal a non-trivial procedure.

In spite of these limitations, the quality and accuracy of the DUACS products makes them valuable for many applications. They are currently used for ~~derivated~~derived oceanographic product~~s~~ generation such as~~like~~ ocean indicators (e.g., regional MSL; ENSO; Kuroshio among others; http://www.aviso.altimetry.fr). They are also currently used for the generation of L~~l~~agrangian products, for which the precision of the current can strongly ~~impacts~~ affect~~s~~ the results (d'Ovidio et al, 2015).

In order to ensure the best ~~homogeneity~~ consistency and quality, the DUACS DT SLA products will be regularly reprocessed for all missions, taking advantage of ~~the~~ new altimeter standards and ~~L3/L4~~ improved L3/L4 processing. The next reprocessed version of the products will be undertaken~~performed~~ as part as the new European Copernicus Marine Environment Marine Service (CMEMS) and is expected for release in 2018.

Appendix A: How to change the reference period

The gridded SLA products can be referenced to another reference period following ~~the~~ Eq. (1), where P and N are two different reference periods and $\langle SLA \rangle_X$ is the temporal mean of the SLA over the period X. In the same way, MSS and MDT can be referenced to different reference periods following eq (2) and (3).

$$SLA_P = SLA_N - \langle SLA_N \rangle_P \qquad (1)$$

$$MSS_P = MSS_N + \langle SLA_N \rangle_P \qquad (2)$$

$$MDT_P = MDT_N + \langle SLA_N \rangle_P \qquad (3)$$

By definition, the ADT is independent of the reference period. ADT is obtained combining SLA and MDT defined over the same reference period (eq. 4)

$$ADT = SLA_N + MDT_N = SLA_P + MDT_P \qquad (4)$$

Appendix B: Description of the OI mapping methodology ~~description~~

The mapping method is a global suboptimal space-time objective analysis which takes into account along-track correlated errors, as described in many previous publications (see for instance Ducet et al., 2000; Le Traon et al., 2003).

The best least squares linear estimator θ_{est} and the associated error field e^2 are given by Bretherton et al. (1976).

$$\theta_{est} = \sum_{i=1}^{n}\sum_{j=1}^{n} A_{ij}^{-1} C_{xj} \Phi_{obs}$$

$$e^2 = C_{xx} - \sum_{i=1}^{n}\sum_{j=1}^{n} C_{xi} C_{xj} A_{ij}^{-1}$$

Where Φ_{obs} is the observation, i.e., the true SLA Φ_i and its observation error ε_i. A is the covariance matrix of the observation and C is the covariance between observation and the field to be estimated.

$$A_{ij} = \langle \Phi_{obs} \Phi_{obs} \rangle = \langle \Phi_i \Phi_j \rangle + \langle \varepsilon_i \varepsilon_j \rangle$$

$$C_{xi} = \langle \theta(x) \Phi_{obs} \rangle = \langle \theta(x) \Phi_i \rangle$$

The spatial and temporal correlation scales (zero crossing of the correlation function) and propagation velocities characteristic of the signal to be retrieved are defined by the function *C(r,t)* as in Arhan and Colin de Verdière (1985).

$$C(r,t) = \left[1 + ar + \frac{1}{6}(ar)^2 - \frac{1}{6}(ar)^3\right] e^{-ar} e^{-t^2/T^2}$$

Where

$$a = 3.337$$

$$r = \sqrt{\left(\frac{dx - C_{px}dt}{L_x}\right)^2 + \left(\frac{dy - C_{py}dt}{L_y}\right)^2}$$

dx, dy and dt define the distance in space (zonal and meridional directions) and time to the point under consideration~~considered~~. The spatial and temporal correlation scales are defined as the first zero crossing of C. T is the temporal correlation radius, L_x and L_y are the spatial~~ee~~ correlation radii~~us~~ (zonal and meridional directions), and C_{px} and C_{py} are the propagation velocities (zonal and meridional directions). The values of the different correlation scales are presented in Sect. 2.2.1

For each grid point where SLA is estimated, the altimeter measurements are selected in a spatial and temporal subdomain defined as 3 times the prescribed spatial and temporal correlation scales~~ prescribed~~. M~~The m~~easurements located outside the smaller subdomain, defined by the spatial and temporal correlation scales, are used to correct for long wavelength errors, enabling us to separate long wavelength errors from the ocean signal. In order to limit the size of the matrix to be inverted, the SLA measurements are subsampled when located outside the smaller subdomain. In that case only one point out of four is retained. Additionally, the matrix A is constructed on~~in~~ a coarse-resolution grid of 1°x1°. The same matrix is used to compute the SLA and associated errors in the surrounding points located on the ¼°x1/4° grid.

The selected measurements ~~selected ~~are centered. The removed mean ~~removed ~~is computed using weights corresponding to the long wavelength error variance defined along each altimeter track. The removed mean SLA value ~~removed ~~is then added back after the analysis.

The observation errors that are considered consist of~~in~~ two components. First, an uncorrelated component is evaluated~~considered~~. Its variance b^2 contributes to the $\langle \varepsilon_i \varepsilon_j \rangle$ ~~matrix ~~diagonal matrix. Then, long-wavelength correlated errors are also considered. In this~~that~~ case, the corresponding variance E_{LW} is added to the non diagonal terms of the $\langle \varepsilon_i \varepsilon_j \rangle$ matrix, as follows:

$\langle \varepsilon_i \varepsilon_j \rangle = \delta_{i,j} b^2 + E_{LW}$ for points i and j that are on the same track and in the same cycle.

$\delta_{i,j}$ is the Kronecker delta.

The variances b^2 and E_{LW} are described in Sect. 2.2.1

Appendix C: Change of the grid spatial resolution between DT2010 and DT2014

Compared to the historical 1/3°x1/3° Mercator native resolution, the Cartesian ¼°x1/4° projection leads to a higher grid resolution between latitudes in the approximare range ~~of nearly~~ ±41.5°N, as illustrated in Fig. C1. These latitudes include the bulk ~~main part~~ of the high variability mesoscale~~s~~ regions~~areas~~, such as~~like~~ the Gulf Stream, Kuroshio, Agulhas current and n~~N~~orth of the confluence area. Above~~Up to~~ these latitudes, the meridionala~~n~~ grid resolution is reduced in the Cartesian projection.

As discussed in Sect. 2.2.1, the grid resolution does not correspond to the spatial scales of the features that are resolved by the DT2014 SLA field.

Acknowledgements

The DT2014 reprocessing exercise has been supported by the French SALP/CNES project with co-funding from the European MyOcean-2 and MyOcean Follow On projects. The datasets are available from~~on~~ the Aviso website (http://aviso.altimetry.fr/) and the CMEMS web site (http://marine.copernicus.eu/~~http~~). Level 2 (GDR) input data are provided by CNES, ESA, NASA. The altimeter standards used in DT2014 were selected taking advantage of the work performed during~~in~~ the first phase of the Sea Level Climate Change Initiative (SL_cci) led by ~~the~~ ESA in 2011-2013.

References

Ablain, M., . Cazenave, G. Valladeau, and S. Guinehut, A new assessment of the error budget of global mean sea level rate estimated by satellite altimetry over 1993-2008. Ocean Science, 5, 193-201, 2009.

Ablain M., A. Cazenave, G. Larnicol, M. Balmaseda, P. Cipollini, Y. Faugère, M. J. Fernandes, O. Henry, J. A. Johannessen, P. Knudsen, O. Andersen, J. Legeais, B. Meyssignac, N. Picot, M. Roca, S. Rudenko, M. G. Scharffenberg, D. Stammer, G. Timms, and J. Benveniste, Improved sea level record over the satellite altimetry era (1993–2010) from the Climate Change Initiative project, Ocean Science., 11, 67-82, doi:10.5194/os-11-67-2015, 2015.

Arbic B. K, Scott R. B., Chelton D. B., Richman J. G. and Shriver J. F., Effects on stencil width on surface ocean geostrophic velocity and vorticity estimation from gridded satellite altimeter data, J. Geophys. Res., vol117, C03029, doi:10.1029/2011JC007367, 2012.

Arhan, M., and A. Colin de Verdiere, Dynamics of eddy motions in the eastern North Atlantic, J. Phys. Oceanogr., 15, 153-170, 1985.

~~AVISO~~Aviso/DUACS, A new version of SSALTO/Duacs products available in April 2014. Technical note. Available at http://www.aviso.altimetry.fr/fileadmin/documents/data/duacs/Duacs2014.pdf, last access: 2015/12/07, 2014a.

~~AVISO~~Aviso/DUACS, User Handbook Ssalto/Duacs: M(SLA) and M(ADT) Near-Real Time and Delayed-Time, SALP-MU-P-EA-21065-CLS, edition 4.1, May 2014, available at http://www.aviso.altimetry.fr/fileadmin/documents/data/tools/hdbk_duacs.pdf, last access: 2015/12/07, 2014b.

Aviso/SALP, Jason-2 validation and cross calibration activities (Annual report 2014) Jason-2 validation and cross calibration activities (Annual report 2014), edition 1.1, January 2015, available at http://www.aviso.altimetry.fr/fileadmin/documents/calval/validation_report/J2/annual_report_j2_2014.pdf, last access 2016/03/31.

Bretherton, F., R. Davis, and C. Fandry, 1976: A technique for objective analysis and design of oceanographic experiments applied to MODE-73. Deep-Sea Res., 23, 559–582.

Capet A., E. Mason, V. Ross, C. Troupin, Y. Faugere, M.-I. Pujol, A. Pascual, Implications of a Refined Description of Mesoscale Activity in the Eastern Boundary Upwelling Systems, Geophys. Res. Lett., 41, doi:10.1002/2014GL061770, 2014.

Carrere L. and M. Ablain, Major improvement of altimetry sea level estimations using pressure derived corrections based on ERA-interim atmospheric reanalysis, Ocean Sci. Discuss., doi:10.5194/os-2015-112, 2016, in review~~2015, in preparation.~~

Chelton, D.B., M.G. Schlax, R.M. Samelson (2011), Global observations of nonlinear mesoscale eddies, *Prog. Oceanogr.* ,91, 167–216. doi:10.1016/j.pocean.2011.01.002

Chelton D., G. Dibarboure , M.-I. Pujol, G. Taburet , M. G. Schlax, The Spatial Resolution of AVISO Gridded Sea Surface Height Fields, OSTST Lake Constance, Germany, October, 28-31 2014, available at http://meetings.aviso.altimetry.fr/fileadmin/user_upload/tx_ausyclsseminar/files/29Red0900-1_OSTST_Chelton.pdf, 2014

Couhert, A., Cerri, L., Legeais, J.-F., Ablain, M., Zelensky, N. P., Haines, B. J., Lemoine, F. G., Bertiger, W. I., Desai, S. D., and Otten, M.: Towards the 1 mm/y stability of the radial orbit error at regional scales, Adv. Space Res., 55, 2–23, doi:10.1016/j.asr.2014.06.041, 2015.

Dee, D. P., Uppala, S. M., Simmons, A. J., Berrisford, P., Poli, P., Kobayashi, S., Andrae, U., Balmaseda, M. A., Balsamo, G., Bauer, P., Bechtold, P., Beljaars, A. C. M., van de Berg, L., Bidlot, J., Bormann, N., Delsol, C., Dragani, R., Fuentes, M., Geer, A. J., Haimberger, L., Healy, S. B., Hersbach, H., Hólm, E. V., Isaksen, L., Kållberg, P., Köhler, M., Matricardi, M., McNally, A. P., Monge-Sanz, B. M., Morcrette, J.-J., Park, B.-K., Peubey, C., de Rosnay, P., Tavolato, C., Thépaut, J.-N., and Vitart, F.: The ERA-Interim reanalysis: configuration and performance of the data assimilation system, Q. J. R. Meteorol. Soc., 137, 553–597, doi:10.1002/qj.828, 2011

Dibarboure G., M-I. Pujol, F. Briol, P.-Y. Le Traon, G. Larnicol, N. Picot, F. Mertz, P. Escudier , M. Ablain, and C. Dufau, Jason-2 in DUACS: first tandem results and impact on processing and products, Mar. Geod., OSTM Jason-2 Calibration/Validation Special Edition – Part 2 Jason-2 Special Edition – Part 2, (34), 214-241, 2011, doi:10.1080/01490419.2011.584826

F. d'Ovidio, A. Della Penna, T. W. Trull, F. Nencioli, M.-I. Pujol, M.-H. Rio, Y.-H. Park, C. Cotté, M. Zhou, and S. Blain, The biogeochemical structuring role of horizontal stirring: Lagrangian perspectives on iron delivery downstream of the Kerguelen Plateau, Biogeosciences, 12, 5567-5581, 2015

Ducet N., Le Traon P.-Y., Reverdun G., Global high-resolution mapping of ocean circulation from TOPEX/Poseidon and ERS-1 and -2, J. Geophys. Res. 105 (C8), 19,477-19,498, 2000

Dufau C., M. Orstynowicz, G. Dibarboure, R. Morrow, P.-Y. La Traon,~~ (2014)~~: Mesoscale Resolution Capability of altimetry: present & future, J. Geophys. Res, ~~2015~~2016, in review

Dussurget R., F. Birol, R. Morrow and P. De Mey, Fine Resolution Altimetry Data for a Regional Application in the Bay of Biscay, Mar. Geod., 34:3-4, 447-476, 2011

Escudier, R., J. Bouffard, A. Pascual, P.-M. Poulain, and M.-I. Pujol, Improvement of coastal and mesoscale observation from space: Application to the northwestern Mediterranean Sea, Geophys. Res. Lett., 40, 2148–2153, doi:10.1002/grl.50324, 2013.

Fernandes, M. J., Lázaro, C., and Nunes, A. L.: Improved Wet Path Delays for all ESA and Reference altimetric missions, Remote Sens. Environ., in preparation, 2014.

Fieguth P, D. MenemenlisS, T. Ho, A. Willsky, C. Wunch, Mapping Mediterranean Altimeter Data with a Multiresolution OptimalInterpolation Algorithm, J. Atmos. Oceanic Technol., 15,535-546, 1998

Griffin D and M Cahill, Assessment of Cryosat near-real-time sea level anomaly data using HF radar and SST imagery, Oral presentation, OSTST Venise, Italy 2012, available at http://www.aviso.altimetry.fr/fileadmin/documents/OSTST/2012/oral/01_thursday_27/06_NRT_applications/07_NRT_Griffin.pdf, 2012.

Hogg, A. McC., M. P. Meredith, D. P. Chambers, E. P. Abrahamsen, C. W. Hughes, and A. K. Morrison, Recent trends in the Southern Ocean eddy field, J. Geophys. Res. Oceans, 120, 257–267, doi:10.1002/2014JC010470, 2015.

Jayne S., B.Owens, B. Cornuelle, Mapping the ocean's surface circulation from altimetry, Oral presentation, OSTST Boulder USA 2013, available at http://www.aviso.altimetry.fr/fileadmin/documents/OSTST/2013/oral/Jayne.pdf, 2013

Juza M., R. Escudier, A. Pascual, M.-I. Pujol, C. Troupin, B. Mourre, J. Tintoré, Impact of the reprocessed satellite altimetry absolute dynamic topography on the Western Alboran Gyre variability, Advances in Space Research, 2015, in ~~preparation~~review.

Leben R R, G H Born, B N Engebreth, Operational Altimeter Data Processing for Mesoscale Monitoring, Mar. Geod., 25:3–18, 2002

Legeais J.-F., P. Prandi, M. Ablain, Validation of altimeter data by comparison with in-situ T/S Argo profiles, Ref. CLS/DOS/NT/15-007, available at http://www.aviso.altimetry.fr/fileadmin/documents/calval/validation_report/annual_report_insitu_TS_2014.pdf, last access: 2015/12/07, 2015

Legeais, J.-F., Ablain, M., and Thao, S.: Evaluation of wet troposphere path delays from atmospheric reanalyses and radiometers and their impact on the altimeter sea level, Ocean Sci., 10, 893– 905, doi:10.5194/os-10-893-2014, 2014.

J.-F. Legeais P. Prandi, M. Ablain, and S. Guinehut, Analyses of altimetry errors using Argo and GRACE data, Ocean Sci. Discuss., doi:10.5194/os-2015-111, 2016, in review.

Le Traon P.Y. and Hernandez F., Mapping of the oceanic mesoscale circulation: validation of satellite altimetry using surface drifters. J. Atmos. Oceanic Technol., 9, 687-698, 1992.

Le Traon P.-Y., Gaspar P., Bouyssel F., and Makhmara H., Using TOPEX/Poseidon data to enhance ERS-1 data, J. Atmos. Oceanic Technol., 12, 161-170, 1995.

Le Traon, P.-Y., and F. Ogor, 1998: *ERS-1/2* orbit improvement using TOPEX/POSEIDON: The 2 cm challenge. *J. Geophys. Res.*, 103, 8045–8057.

LeTraon P.-Y., G Dibarboure, Mesoscale Mapping Capabilities of Multiple-Satellite Altimeter Missions, J. Atmos. Oceanic Technol., 16, 1208-1223, 1999.

LeTraon P.-Y, Y. Faugere, F. Hernamdez, J. Dorandeu, F. Mertz and M. Abalin, Can We Merge GEOSAT Follow-On with TOPEX/Poseidon and ERS-2 for an Improved Description of the Ocean Circulation?, J. Atmos. Oceanic Technol., 20, 889-895, 2003

Marco M., A. Pascual, M-I Pujol, Improved satellite altimeter mapped sea level anomalies in the Mediterranean Sea: A comparison with tide gauges, Advances in Space Research 56 (4), 596–604. doi:10.1016/j.asr.2015.04.027, 2015

Mulet S., M.H. Rio, E. Greiner, N. Picot, A. Pascual, New global Mean Dynamic Topography from a GOCE geoid model, altimeter measurements and oceanographic in-situ data, OSTST Boulder USA 2013, available at http://www.aviso.altimetry.fr/fileadmin/documents/OSTST/2013/oral/mulet_MDT_CNES_CLS13.pdf, 2013.

Ollivier, A., Faugère, Y., Picot, N., Ablain, M., Femenias, P., and Benveniste, J.: Envisat Ocean Altimeter Becoming Relevant for Mean Sea Level Trend Studies, Mar. Geodesy, 35, 118–136, 2012.

Pascual A., Faugere Y., Larnicol G., Le Traon P.-Y., Improved description of the ocean mesoscale variability by combining four satellite altimeters, Geophys. Res. Lett., 33(2), doi:10.1029/2005GL024633, 2006

Philipps S., H. Roinard, N. Picot, Jason-2 reprocessing impact on ocean data (cycles 001 to 145), Ref. CLS/DOS/NT/12-222., available at http://www.aviso.altimetry.fr/fileadmin/documents/calval/validation_report/J2/Jason2ReprocessingReport-v2.1.pdf, last access: 2014/12/07, 2013a.

Philipps S., H. Roinard, N. Picot, (2013b): Jason-1 validation and cross calibration activities [Annual Report 2013], Ref. CLS/DOS/NT/13-226., available at http://www.aviso.altimetry.fr/fileadmin/documents/calval/validation_report/annual_report_j1_2013.pdf, last access: 2014/07/25, 2013b.

Pujol M.-I. and G. Larnicol, Mediterranean Sea eddy kinetic energy variability from 11 years of altimetric data, J. Mar. Syst., 58 (3–4) (2005), 121–142, 2005.

Ray R.D. and Zaron E.D., M2 internal tides and their observed wavenumber spectra from satellite altimetry, Journal of Physical Oceanography, doi: 10.1175/JPO-D-15-0065.1, in press., 2015.

Rio, M. H., S. Guinehut, and G. Larnicol, New CNES-CLS09 global mean dynamic topography computed from the combination of GRACE data, altimetry, and in-situ measurements, J. Geophys. Res., 116, C07018, doi:10.1029/2010JC006505, 2011.

Rio, M-H, Use of altimeter and wind data to detect the anomalous loss of SVP-type drifter's drogue. J. Atmos. Oceanic Technol., DOI:10.1175/JTECH-D-12-00008.1, 2012.

Schaeffer P., Y. Faugere, J. F. Legeais, A. Ollivier, T. Guinle, N. Picot, The CNES CLS11 Global Mean Sea Surface Computed from 16 Years of Satellite Altimeter Data. Mar. Geod., Special Issue, Jason-2, Vol.35, 2012.

Scharroo, R. and Smith,W. H. F.: A global positioning system based climatology for the total electron content in the ionosphere, J. Geophys. Res., 115, A10318, doi:10.1029/2009JA014719, 2010

Taylor, K. E., Summarizing multiple aspects of model performance in a single diagram, J. Geophys. Res., 106(D7), 7183–7192, doi:10.1029/2000JD900719, 2001.

Valladeau G., J.-F. Legeais, M. Ablain, S. Guinehut, N. Picot, Comparing Altimetry with Tide Gauges and Argo Profiling Floats for Data Quality Assessment and Mean Sea Level Studies, Marine Geodesy, OSTM Jason-2 Applications Special Edition – Part 3, (35), 42-60, doi:10.1080/01490419.2012.718226, 2012

Prandi P., G. Valladeau G., M. Ablain, Validation of altimeter data by comparison with tide gauge measurements, Ref. CLS/DOS/NT/15-020, available at http://www.aviso.altimetry.fr/fileadmin/documents/calval/validation_report/annual_report_insitu_TG_2014.pdf, last access: 2015/12/07, 2015.

Rudenko, S., Otten, M., Visser, P., Scharroo, R., Schöne, T., and Esselborn, S.: New improved orbit solutions for the ERS-1 and ERS-2 satellites, Adv. Space Res., 49, 1229–1244, 2012.

Table 1: Variance of the differences between gridded DT2014 two-sat-merged products and independent TPN along-track measurements for different geographic selections (unit = cm²). In parenthesis: variance reduction (in %) compared with the results obtained with the DT2010 products. Statistics are presented for wavelengths ranging between 65-500 km and after latitude selection (|LAT| < 60°).

	TPN [2003,2004]
Reference area*	1.4 (-0.7%)
Dist coast > 200km & variance < 200 cm²	4.9 (-2.1%)
Dist coast > 200km & variance > 200 cm²	32.5 (-9.9%)
Dist coast < 200km	8.9 (-4.1%)

**The reference area is defined by [330,360°E]; [-22,-8°N]*

Table 2: Taylor skill scores for ~~of~~ the comparison of the geostrophic currents computed~~deduced~~ from altimetry or measured by drifters. Results obtained with DT2014 (2010) products are in bold (parenthese~~i~~s).

	Zonal	Meridian
Outside the equatorial band	**0.83** (0.82)	**0.62** (0.63)
Inside the equatorial band	**0.87** (0.85)	**0.83** (0.81)

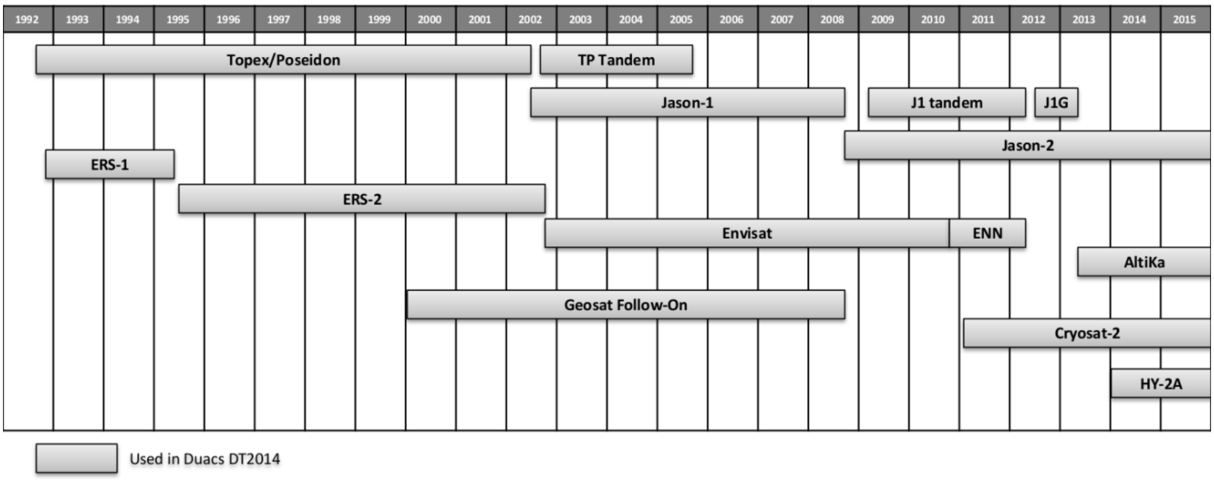

Figure 1 : Timeline of the altimeter missions used (or expected) in the multi-mission DUACS DT system.

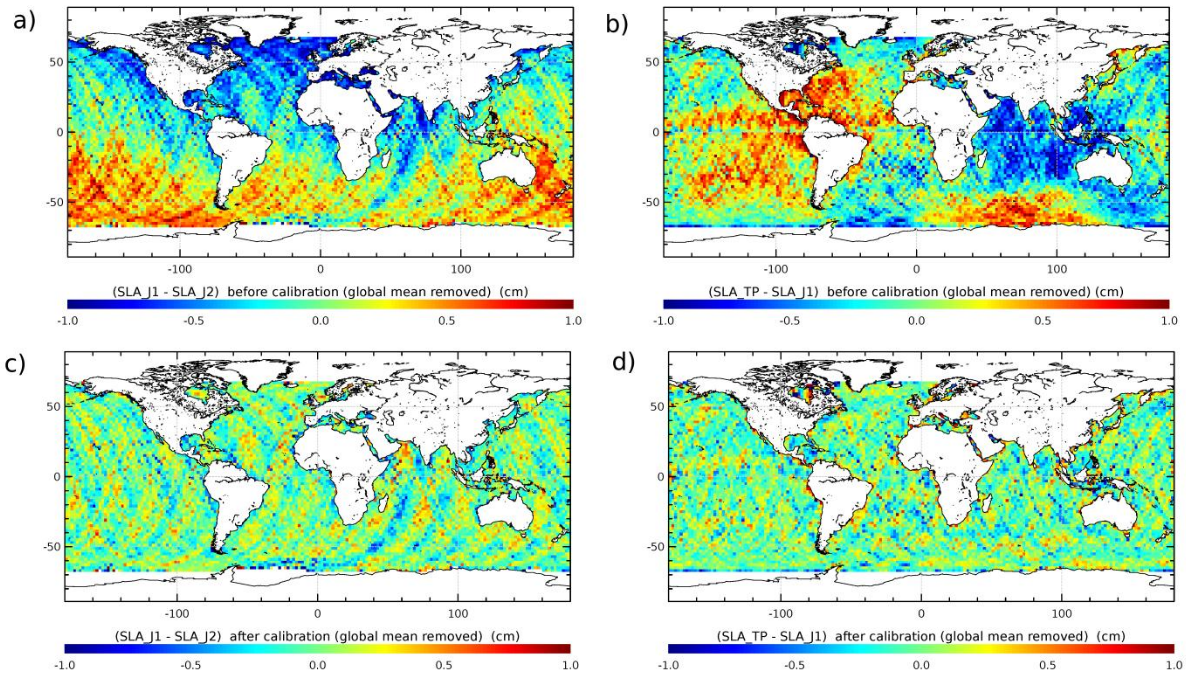

Figure 2 : Regional SLA biases observed between TP and J1 during the cycles 1 to 21 of J1 before (a) and after (c) reduction of ~~the~~ biases. Regional SLA biases observed between J1 and J2 during ~~the~~ cycles 1 to 21 of J2, before (b) and after (d) reduction of ~~the~~ biases.

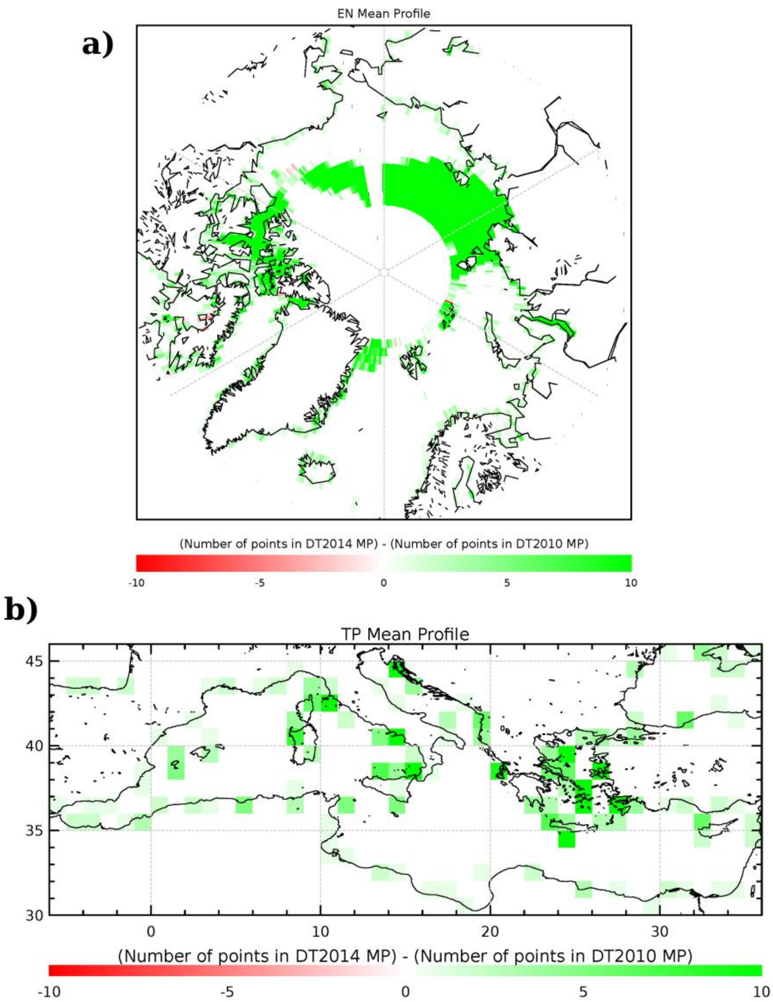

Figure 3: Differences of the number of points defined along the ~~new~~ DT2014 and ~~old~~ DT2010 versions of the Mean Profile defined along theoretical EN (a) and TP (b) ~~theoretical~~ tracks. Statistics done in 1°x1° boxes.

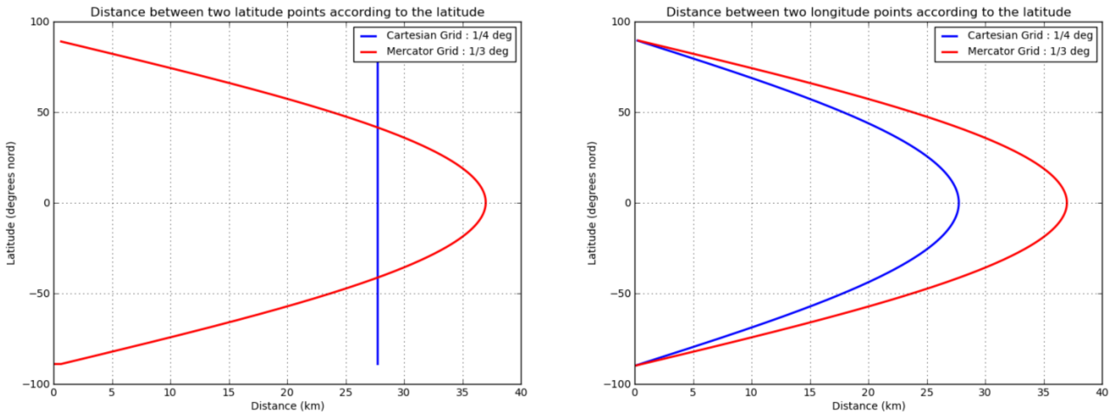

~~Figure 4 : Left : Difference between two successive grid points on a meridian section as a function of the latitude, for a 1/4°x1/4° Cartesian resolution (blue) and 1/3°x1/3° Mercator resolution (red). Right: same as left but for a zonal section.~~

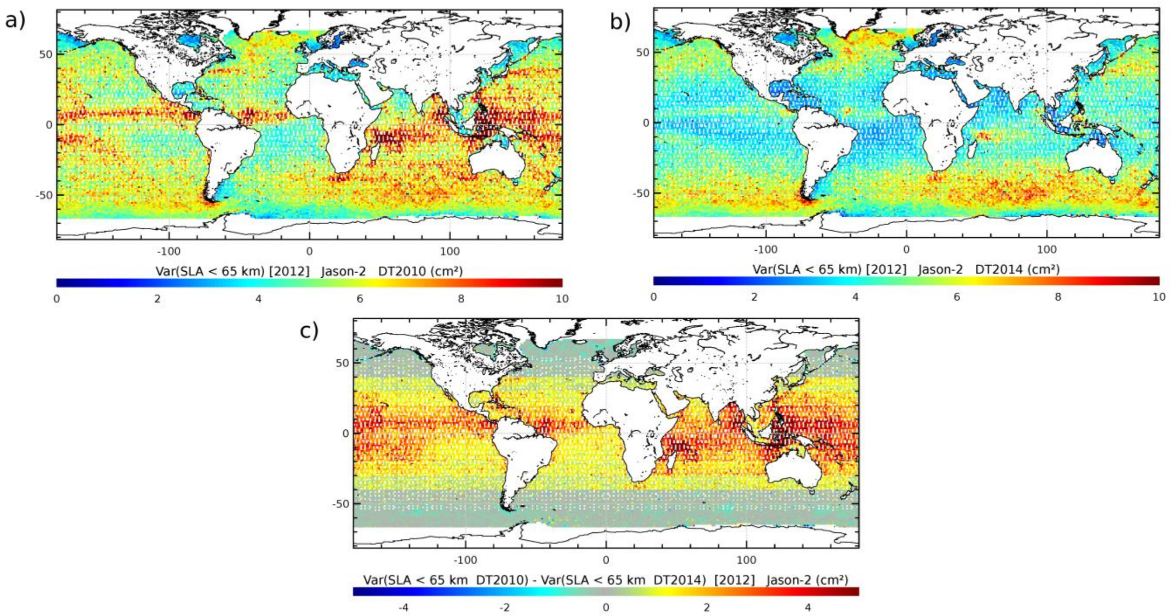

Figure 4~~5~~ : Variance of the short wavelength signal ~~filtered~~ removed (by low-pass filtering) on L3 along-track J2 ~~products~~ SLA in the DT2010 (a) and DT2014 (b) versions. c) Differences between ~~the two maps (c~~a) and b)~~)~~. Statistics done over year 2012.

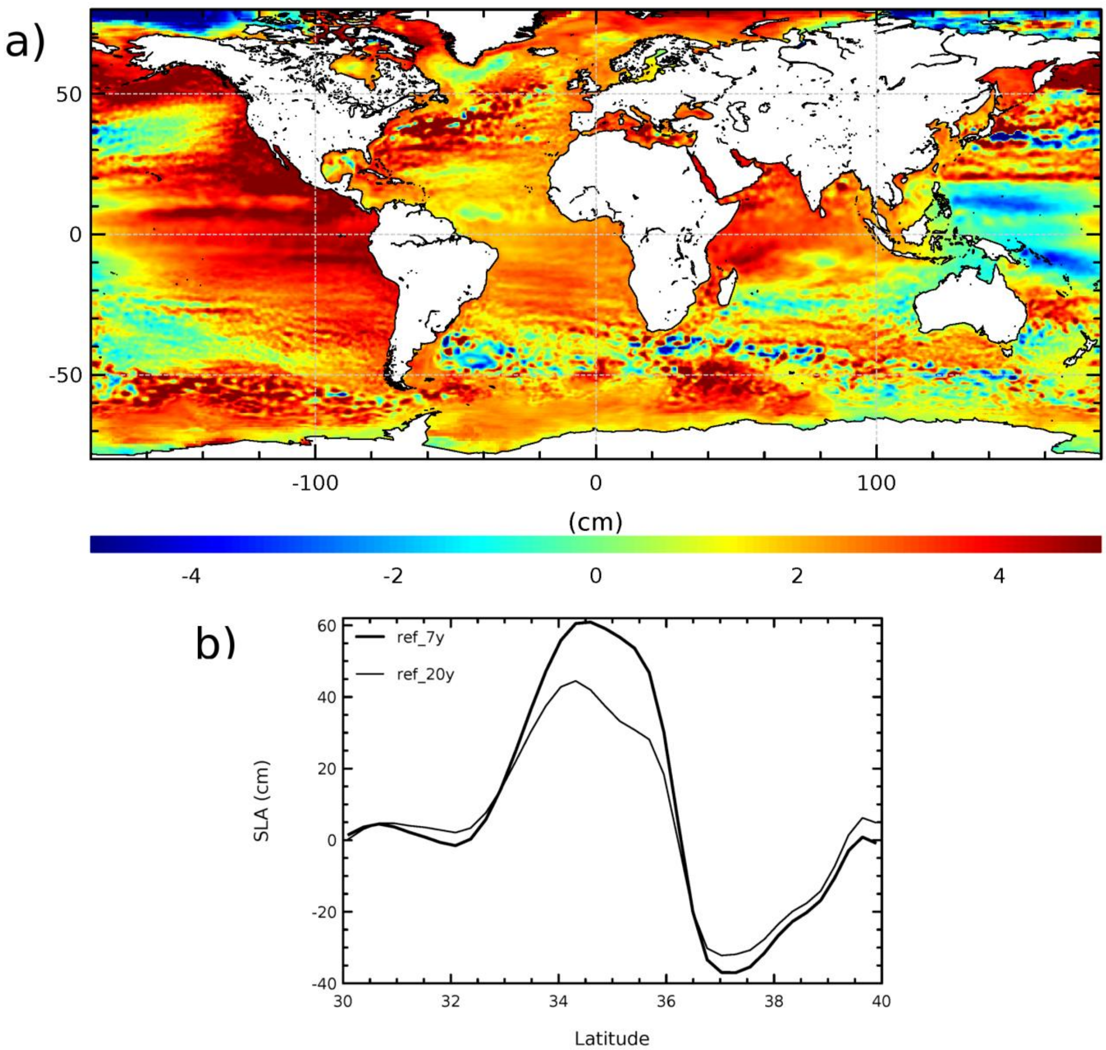

Figure 5~~6~~ : Impact of the change of reference period. a) regional MSL variation differences when considering the 7-year or the 20-year period. b) SLA along a J2 track crossing the Kuroshio, referenced to the 7-year (~~red~~thick line) and 20-year (~~bleu~~thin line) period.

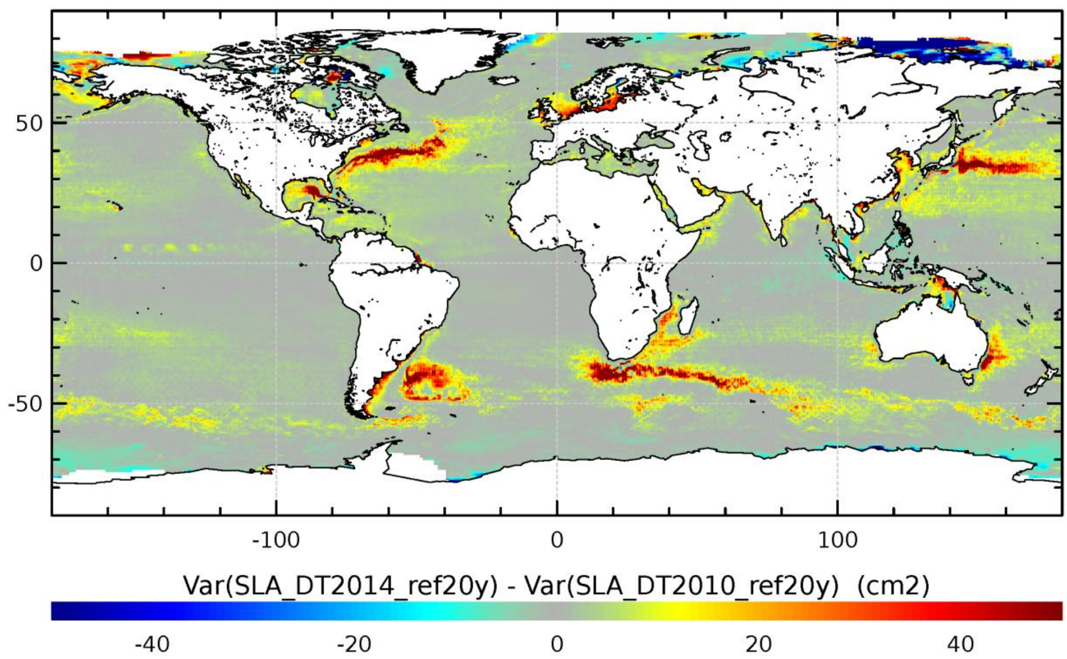

Figure ~~7~~6: Difference between SLA variance observed with DT2014 gridded products and SLA variance observed with DT2010 products over the [1993, 2012] period. Gridded products merging all the altimeters available are considered (i.e., “all-sat-merged” in DT2014; “UPD” in DT2010). DT2010 products were referenced to the 20-year altimeter reference period and interpolated onto the ¼°x1/4° Cartesian grid for comparison with DT2014.

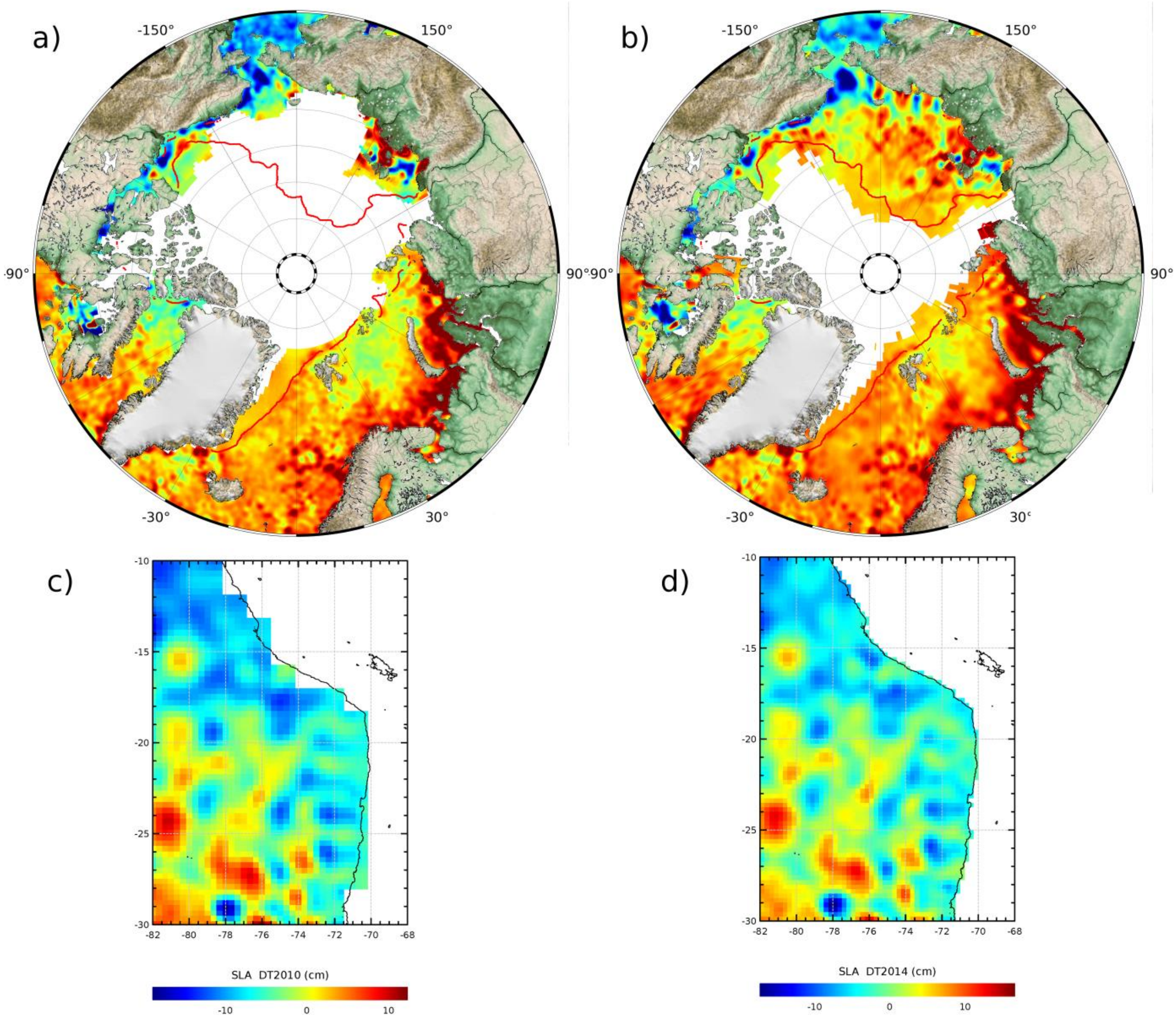

Figure 7~~8~~: Coverage improvement associated with the DT2014 reprocessing. Map of SLA for day 2011/10/17 over the Arctic Ocean observed with the DT2010 (a) and DT2014 (b) products. Sea ice extent~~edge~~ is ~~underlined~~ shown with red line (OSISAF product). Same map along the w~~W~~estern South~~-~~ American coast with DT2010 (c) and DT2014 (d).

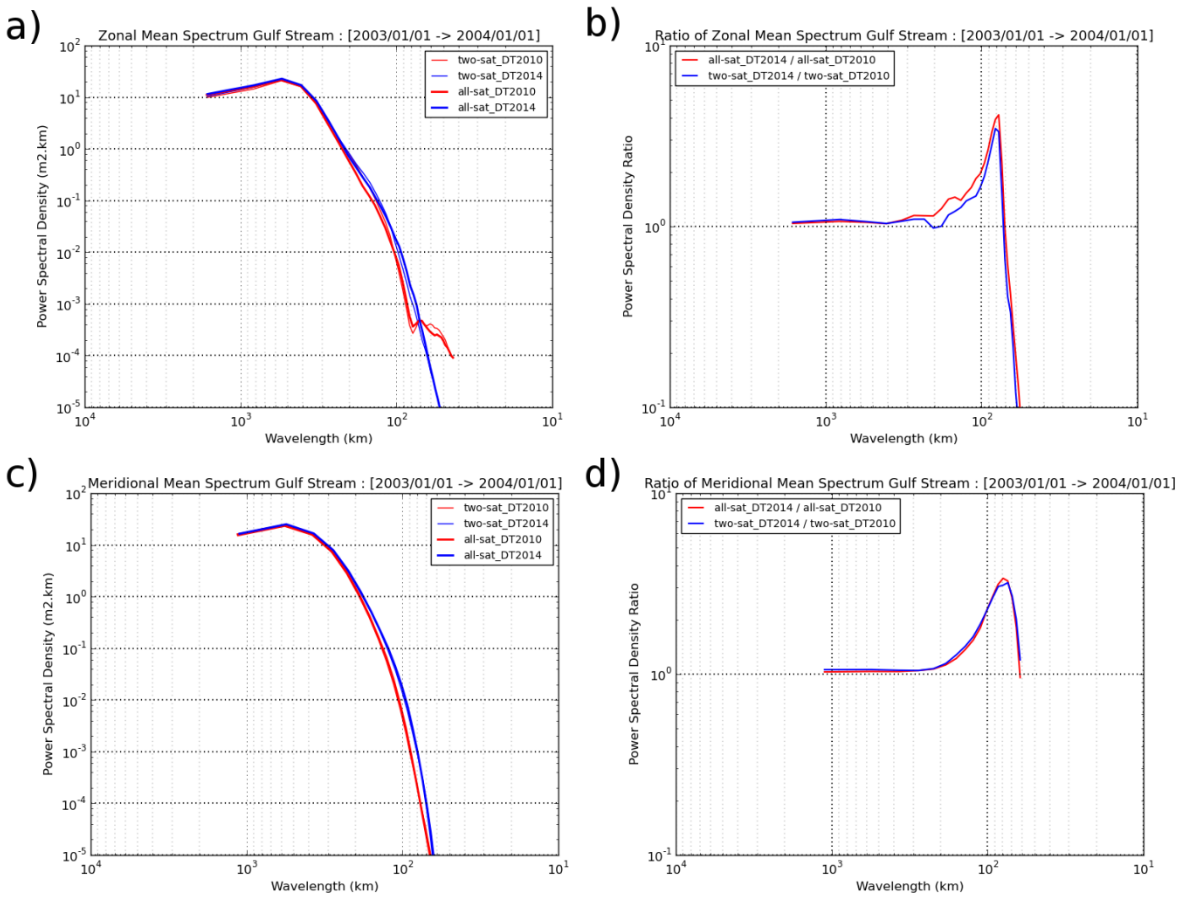

Figure 8~~9~~: Mean zonal (a) and meridio~~a~~nal (c) power spectral density (PSD) computed~~deduced~~ from gridded DT2014 (blue) and DT2010 (red) all-sat-merged (UPD; thick line) and two-sat-merged (REF; thin line) ~~products~~ SLA fields over the Gulf Stream area during ~~the year~~ 2003 (when the constellation included J1, TP Tandem, Geosat Follow On and EN). Ratio between DT2010 and DT2014 ~~products~~ PSD when all-sat-merged (UPD; ~~thick~~ red line) and two-sat-merged (REF; ~~thin~~ bl~~e~~ue line) are considered: zonal (b) and meridional~~an~~ (d) components~~.~~.

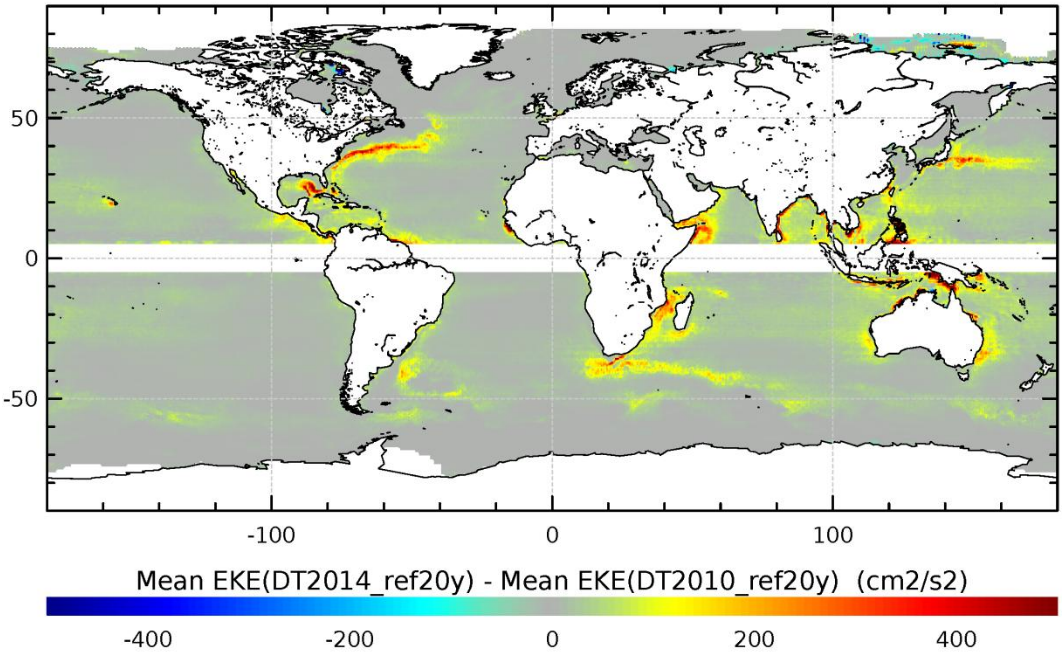

Figure 9~~10~~: Difference of the mean EKE ~~between~~ computed~~deduced~~ from DT2014 and DT2010 ~~products~~ SLA over the [1993, 2012] period. Gridded ~~products~~ SLA merging ~~of~~ all the altimeters available are considered (i.e., “all-sat-merged” in DT2014; “UPD” in DT2010). DT2010 ~~products~~ SLA was~~were~~ referenced to the 20-year altimeter reference period and interpolated onto a~~the~~ ¼°x1/4° Cartesian grid for comparison with DT2014. The s~~S~~ame methodology (c~~C~~entered d~~D~~ifferences) was used for geostrophic current computations for ~~both~~ DT2010 and DT2014.

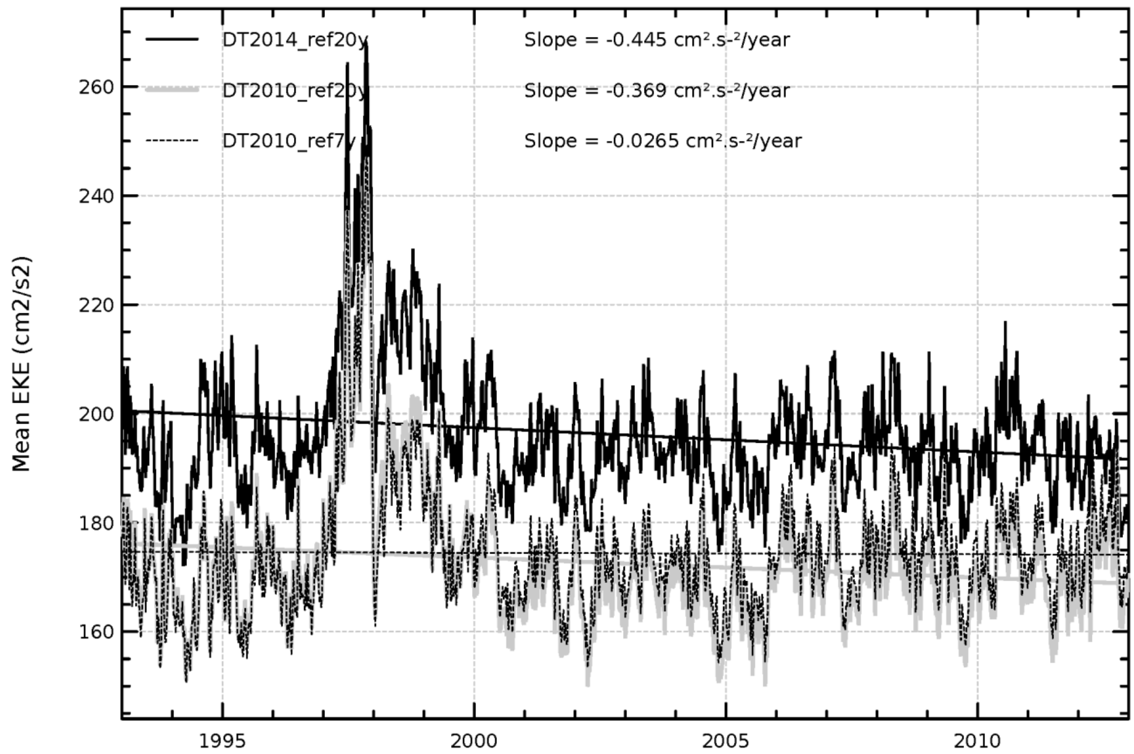

Figure 10~~11~~: Evolution of the mean EKE over the global ocean (selection of latitudes lower than 60°), computed~~deduced~~ from the DT2014 ~~reprocessed product~~ (black line) and ~~the previous~~ DT2010 ~~version~~ SLA gridded products referenced to~~on~~ the 20-year period (black dotted~~s~~ lines) or to~~on~~ the 7-year period (grey ~~dotteds~~ lines). The s~~S~~ame methodology (f~~F~~inite d~~D~~ifferences) was used for the geostrophic current computation for ~~both~~ DT2010 and DT2014.

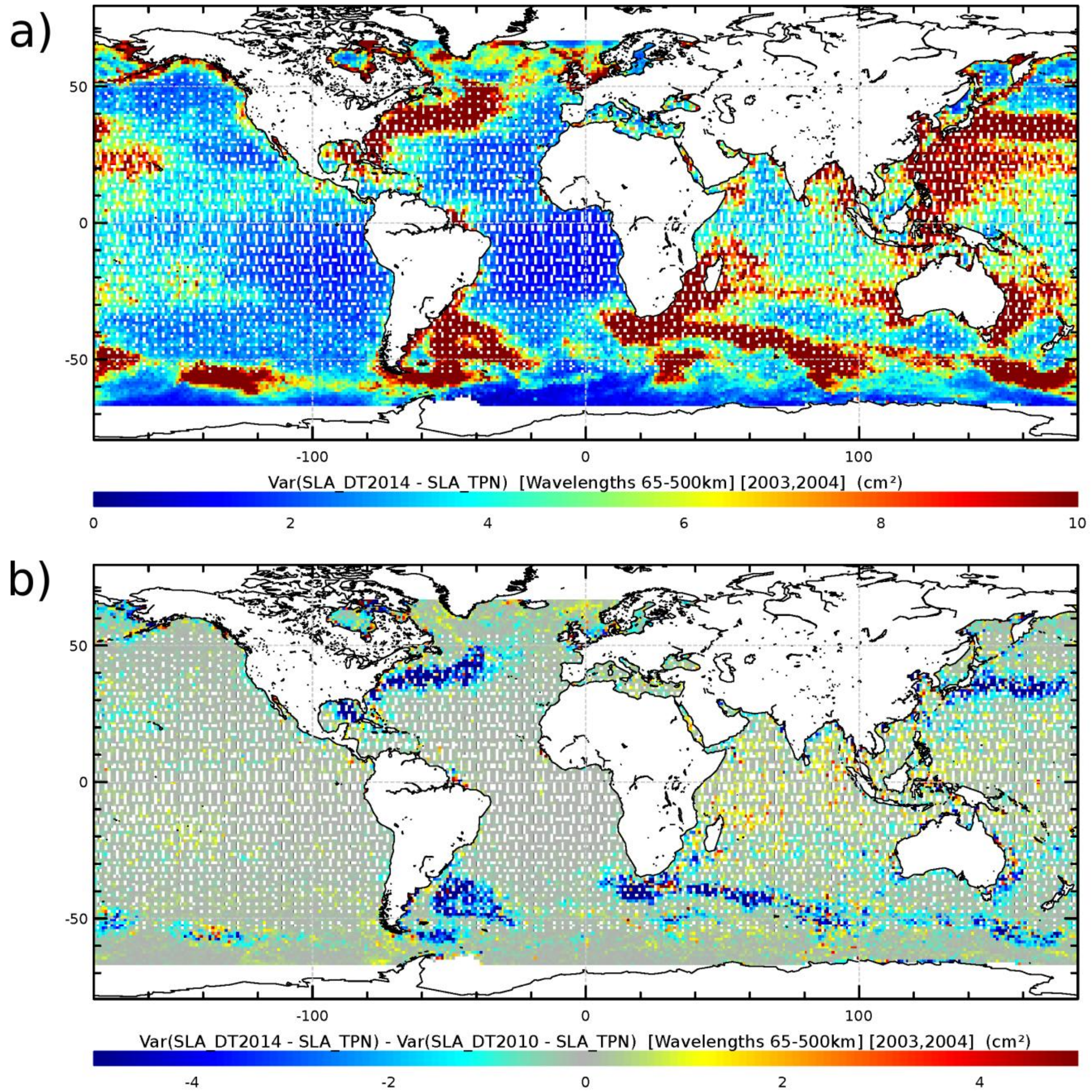

Figure 11~~12~~: a) ~~variance~~ Variance of the differences between gridded DT2014 two-sat-merged ~~products~~ SLA and independent TPN along-track SLA measurements. Statistics are presented for wavelengths ranging from 65-500 km. (unit = cm^2). b) Differences ~~variance reduction compared~~ with the results obtained with the DT2010 SLA products. ~~Statistics are presented for wavelength ranging 65-500 km. (unit = cm^2)~~ Negative values indicate a reduction of the differences between gridded and along-track SLA when DT2014 products are considered.

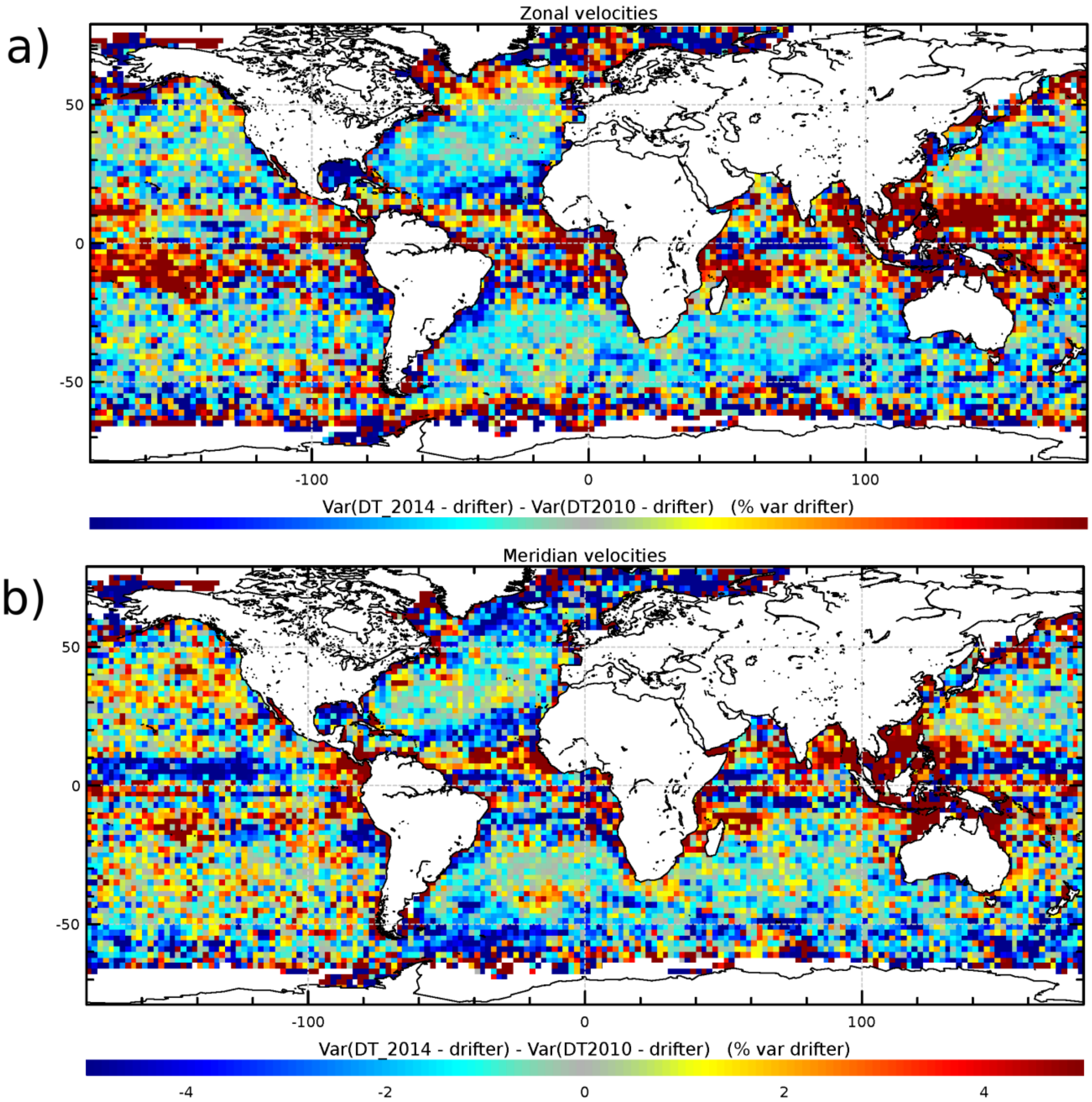

Figure 12~~13~~: Maps of the difference of the variances of the altimeter geostrophic currents minus~~–~~ drifter measurement differences, using successively DT2014 and DT2010 SLA gridded products.~~Variance reduction of the geostrophic current differences between altimeter gridded products and drifters measurements, when using DT2014 rather than DT2010 products.~~ The ~~variance reduction~~ difference of variance is expressed in % of the drifter variance. Zonal (a) and m~~M~~eridional~~an~~ (b) component differences. Negative values mean~~s~~

that the variance of the differences between geostrophic currents ~~deduced~~ from altimetry and from drifter measurement is reduced when considering the DT2014 product.

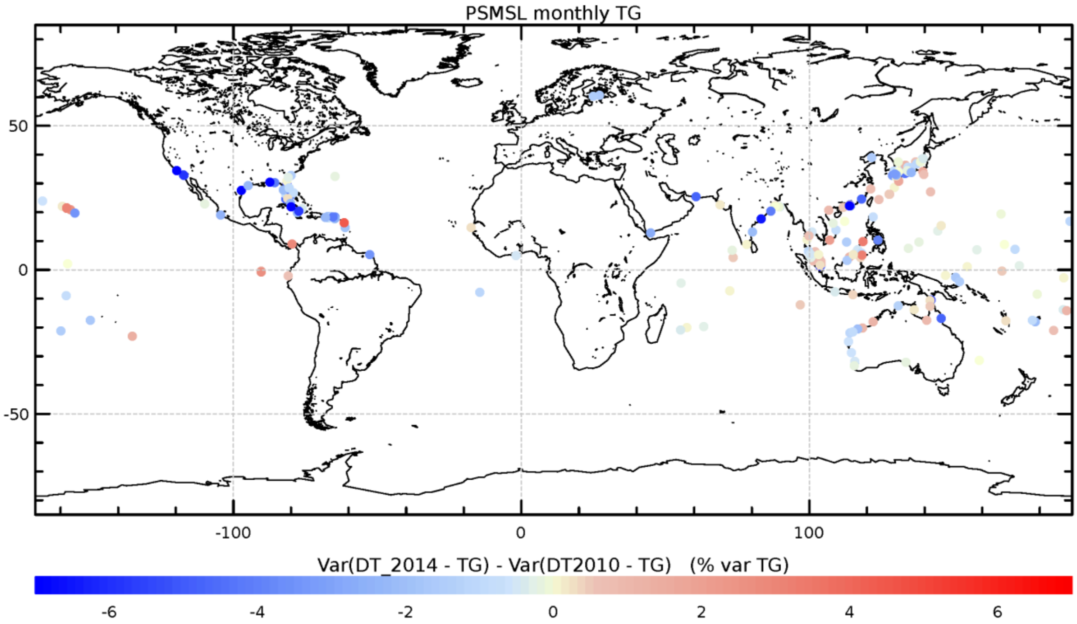

Figure 13~~14~~: Difference of the variance of the altimeter SLA minus~~–~~ tide gauge SLA differences, using successively DT2014 and DT2010 SLA gridded products~~Variance reduction of the sea level differences between altimeter gridded products and tide gauges measurements, when using DT2014 rather than DT2010 products~~. ~~Monthy~~Monthly TG from PSMSL. Negative values mean~~s~~ that the SLA differences between altimetry and tide gauges is reduced when considering DT2014 products.

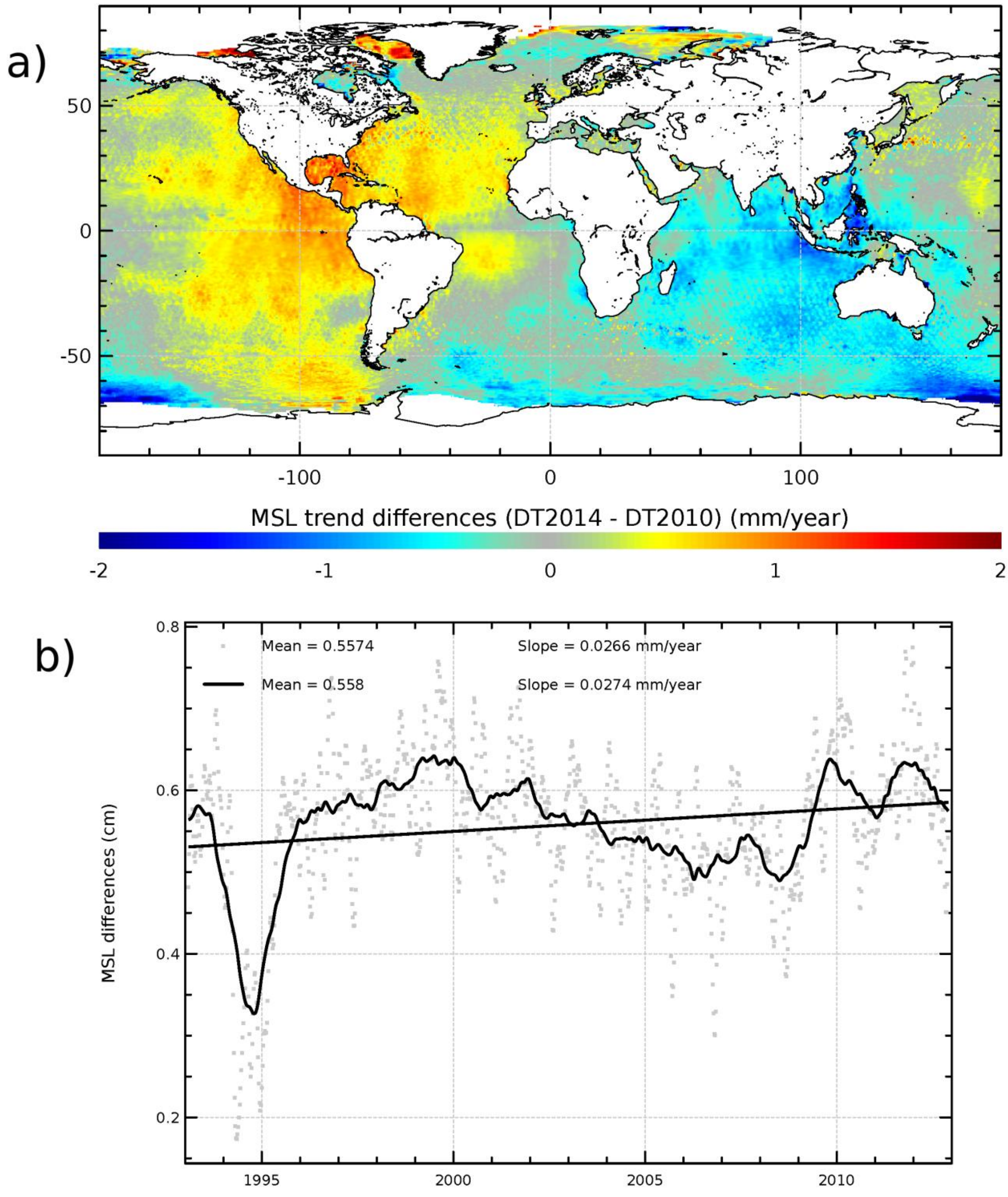

Figure 14~~15~~: a) Map of the differences of the local MSL trend ~~differences~~ estimated from the ~~between~~ DT2014 and DT2010 gridded SLA products. MSL estimated over the [1993, 2012] period. b) Temporal evolution of the differences of the global MSL ~~differences~~ estimated from~~between~~ DT2014 and DT2010.

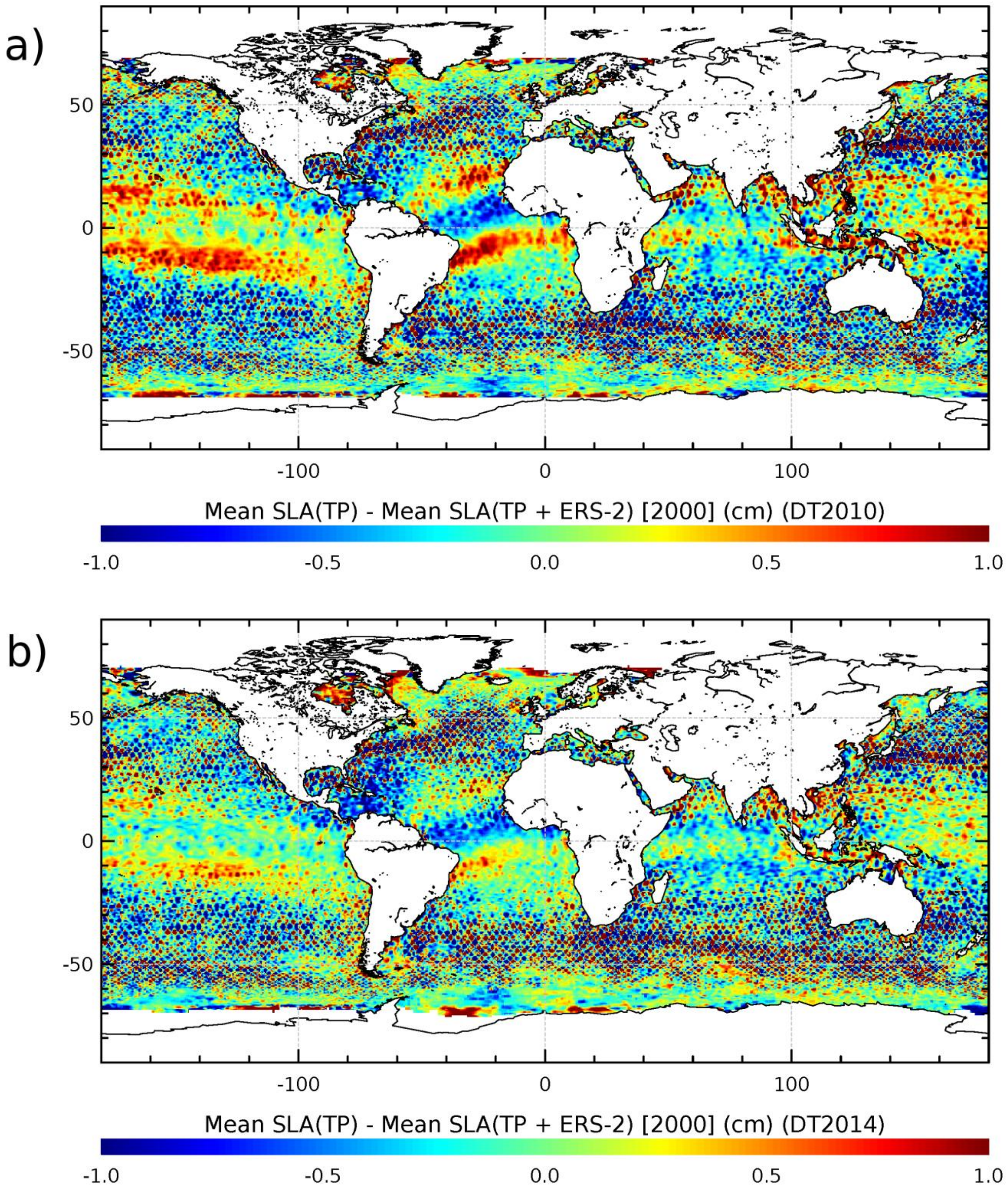

Figure 15~~16~~:~~:~~ Difference of the mean SLA over the year 2000, measured with TP only, and with the merged TP+ERS-2 product. Comparison done for the DT2010 (a) and DT2014 (b) products.

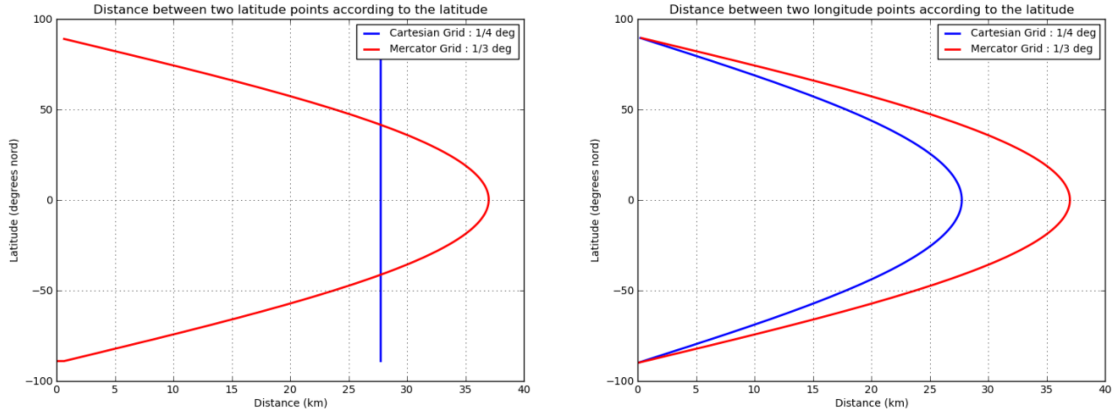

Figure ~~4~~C1 : Left : Difference between two successive grid points on a meridional~~aan~~ section as a function of ~~the~~ latitude, at~~for a~~ 1/4°x1/4° Cartesian resolution (blue) and 1/3°x1/3° Mercator resolution (red). Right: same as left but for a zonal section.